Low-density lipoprotein receptor-related protein-1 (LRP1) mediates autophagy and apoptosis caused by *Helicobacter pylori* VacA

Kinnosuke Yahiro[1], Mamoru Satoh[2], Masayuki Nakano[3], Junzo Hisatune[3,4], Hajime Isomoto[5], Jan Sap[6], Hidekazu Suzuki[7], Fumio Nomura[2], Masatoshi Noda[1], Joel Moss[8], and Toshiya Hirayama[3,*]

Departments of [1]Molecular Infectiology and [2]Molecular Diagnosis, Graduate School of Medicine, Chiba University, Chiba 260-8670, Japan; [3]Department of Bacteriology, Institute of Tropical Medicine, Nagasaki University, Nagasaki 852-8523, Japan; [4]Department of Bacteriology, Hiroshima University Graduate School of Biomedical Sciences, Hiroshima 734-8551, Japan; [5]Department of Gastroenterology and Hepatology, Nagasaki University Hospital, Nagasaki 852-8523, Japan;[6]University Paris Diderot, Sorbonne Paris Cité, Epigenetics and Cell Fate, UMR 7216 CNRS, Paris, France;[7]Division of Gastroenterology and Hepatology, Department of Internal Medicine, Keio University School of Medicine, Tokyo 160-8582, Japan; [8]Cardiovascular and Pulmonary Branch, NHLBI, National Institutes of Health, Bethesda, Maryland 20892, USA

Running title: LRP1 mediates VacA-induced autophagy and apoptosis

Address correspondence to: Toshiya Hirayama. Phone: +81-95-819-7831 Fax:+81-95-819-7877.
E-mail: hirayama@net.nagasaki-u.ac.jp

Keywords: *Helicobacter pylori*, vacuolating cytotoxin (VacA), LRP1, autophagy, apoptosis.

Background: *Helicobacter pylori* VacA receptor(s) responsible for apoptotic cell death and autophagy has not been identified during intoxication.

Results: VacA-induced autophagy via low-density lipoprotein receptor-related protein-1 (LRP-1) binding precedes apoptosis.

Conclusion: LRP1 mediates VacA-induced autophagy and apoptosis.

Significance: This study identified LRP1 as a VacA receptor associated with toxin-induced autophagy and apoptosis and its importance in the processes.

Abstract

In *Helicobacter pylori* infection, vacuolating cytotoxin (VacA)-induced mitochondrial damage leading to apoptosis is believed to be a major cause of cell death. It has also been proposed that VacA-induced autophagy serves as a host mechanism to limit toxin-induced cellular damage. Apoptosis and autophagy are two dynamic and opposing processes that must be balanced to regulate cell death and survival. Here we identify the low-density lipoprotein receptor-related protein-1 (LRP1) as the VacA receptor for toxin-induced autophagy in the gastric epithelial cell line AZ-521, and show that VacA internalization through binding to LRP1 regulates the autophagic process

including generation of LC3-II from LC3-I, which is involved in formation of autophagosomes and autolysosomes. Knockdown of LRP1 and Atg5 inhibited generation of LC3-II as well as cleavage of PARP, a marker of apoptosis, in response to VacA, whereas caspase inhibitor, Z-VAD-FMK, and necroptosis inhibitor, Necrostatin-1, did not inhibit VacA-induced autophagy, suggesting that VacA-induced autophagy via LRP1 binding precedes apoptosis. Other VacA receptors such as RPTPα, RPTPβ, and fibronectin did not affect VacA-induced autophagy or apoptosis. Therefore, we propose that the cell surface receptor, LRP1, mediates VacA-induced autophagy and apoptosis.

Introduction

Helicobacter pylori (*H. pylori*) colonizes more than half the world's population. Although persistent infection by *H. pylori* is accepted as a major cause of gastroduodenal diseases (e.g. the responsible cellular pathways, peptic ulcer disease, gastric lymphoma, gastric adenocarcinoma) have not been defined. Variation in manifestations of *H. pylori* infection in different populations suggests differences in virulence of strains, host genetic susceptibility, and responses to environmental factors. Many *H. pylori* strains isolated from patients contain the *cagA* gene (cytotoxin-associated gene A) as well as produce the vacuolating cytotoxin, VacA. Additional *H. pylori* products, including urease, OipA, adhesins, heat-shock protein, and lipopolysaccharide appear to be involved in virulence **(1,2)**.

Interestingly, VacA causes epithelial damage in mouse models both when given orally as a single agent **(3)** and when delivered by a toxigenic strain of *H. pylori* during gastric infection **(4,5)**. In vitro, VacA is internalized by endocytosis **(6)**, which is inhibited by CagA **(7,8)**, and exerts multiple effects on susceptible cells, including vacuolation and mitochondrial damage, leading eventually to apoptosis **(9-13)** . In addition, VacA forms hexametric pores, followed by endocytosis and processing into late-endosomal compartments**(14),** which then undergo osmotic swelling to become large acidic vacuoles. Although vacuolation is the most obvious effect of VacA in vitro, it is not as obvious in vivo. The pleiotropic effects of VacA appear to result from activation of different signal transduction pathways through binding to several epithelial cell receptors, e.g., receptor protein tyrosine phosphatase (RPTP) β and α **(15,16)**, fibronectin (FN) **(17)**, and sphingomyelin **(18).**

VacA enhanced tyrosine phosphorylation of the G protein-coupled receptor kinase-interactor 1 (Git1) as did pleiotrophin (PTN), an endogenous ligand of RPTPß. **(19)**. Oral administration of VacA to wild-type mice, but not to *RPTPß* KO mice, resulted in gastric ulcer. However, cells lacking RPTPß were able to internalize VacA and undergo vacuolation **(20)**, suggesting that other VacA receptors were responsible for vacuolation. Recent interest has focused on the immunosuppressive effects of VacA, i.e., VacA inhibited proliferation of T

cells due to down-regulation of interleukin-2 (IL-2) transcription **(21,22)**. Through interactions with the β2-integrin subunit CD18 of the leucocyte-specific integrin LFA-1 **(23)**, VacA plays an important role in inhibition of interleukin-2 (IL-2) gene expression after clathrin-independent endocytosis via PKC-dependent phosphorylation of the cytoplasmic tail of CD18 **(24)**. Thus, VacA has effects on both epithelial cells **(25)** as well as inflammatory cells **(26)**.

Over the last 10 years, studies have focused on the mechanism of cell death resulting from mitochondrial damage caused by VacA **(10,12,13,27)**. Additional recent studies have shown that VacA induces autophagy, but the pathway has not been identified **(28,29)**. Autophagy can promote the survival of dying cells **(30)**. However, increased autophagic activity can also lead to cell death **(31-35)**, suggesting that autophagy can be responsible for both cytoprotective and cytotoxic activities, depending on the specific cellular conditions.

Here we purified from AZ-521 cells, a human gastric epithelial ell line, a surface membrane protein, p500, which binds VacA, and identified it as low-density lipoprotein receptor-related protein-1 (LRP1). LRP1 binding of VacA was shown to be specifically responsible for VacA-induced autophagy and apoptosis. Similar to RPTPα and RPTPß, LRP1 mediates VacA internalization in AZ-521 cells, but in contrast to RPTPα and RPTPß, LRP1 targeted downstream pathways leading to autophagy and apoptosis.

Experimental and procedures

Antibodies and other reagents

Anti-LC3B, anti-cleaved caspase-7, anti-cleaved PARP, anti-Beclin-1 and anti-mTOR antibodies were from Cell Signaling. Mouse monoclonal antibodies reactive with LRP1 (8G1) were from Santa Cruz Biotechnologies; those reactive with RPTPβ were from BD Biosciences; and those reactive with LC3 (clone 1703) were from Cosmo Bio. Anti-RPTPβ antibody was raised against its extracellular domain, corresponding to the N-terminal amino acids of the human protein **(36)**. Anti-RPTPα rabbit polyclonal antibodies for immunoblotting were provided by Dr. Jan Sap and anti-RPTPα rabbit polyclonal antibodies for immunofluorescence experiments were raised against its extracellular domain, corresponding to the N-terminal amino acids of the human protein; mouse monoclonal antibodies reactive with α-tubulin, necrostatin-1 and 5-nitro-2-(3-phenylpropylamino)benzoic acid (NPPB) were from Sigma Aldrich. Diamidino-2-phenylindole dihydrochloride (DAPI) and 4,4′-disothiocyanatostibene-2,2′-disulfonic acid (DIDS) were from Invitrogen. A general caspase inhibitor, Z-VAD-FMK was from BD Pharmingen. 3-methyladenine (3-MA) was from MP Biomedicals.

Cell culture and gene silencing

AZ-521 cells, a human gastric cancer cell line obtained from the Japan Health Sciences Foundation, were cultured in Earle's minimal essential medium (Sigma) containing 10% fetal calf serum. AGS cells, a human gastric cancer

cell line, were cultured in RPMI1640 (Sigma) containing 10% fetal calf serum. Cells were plated into 24-well dishes (5×10^4 cells /well) or 12-well dishes (1×10^5 cells /well) in EMEM containing 10% FCS. RNA interference-mediated gene knockdown was performed using validated Qiagen HP small-interfering RNAs (siRNAs) for mTOR (SI00300244). The validated LRP1 siRNA was purchased from Ambion. Beclin-1 siRNA was designed and validated as described by Hoyer-Hansen et al. **(37)**. Atg5 siRNAs (Atg5-1, agugaacaucugagcuacccggaua; Atg5-2, caaucccauccagaguugcuuguga) were designed and validated as described by Yang et al. **(38)** RPTPβ siRNA (5'-gcacaagaaucgauaacaua-3') and RPTPα siRNA (5'-cgaagagaauacagacuau-3') were synthesized by B-Bridge. Negative-control siRNAs were purchased from Sigma Aldrich. AZ-521 cells were transfected with 100 nM of the indicated siRNAs for 48-72 h using Lipofectamine™ RNAiMax transfection reagent (Invitrogen) according to the manufacturer's protocol. Knockdown of the target proteins was confirmed by immunoblotting with the indicated antibodies.

RPTPα shRNA expression vector construction and transfection

The three highest scoring shRNA sequences targeted for human RPTPα were chosen by B-Bridge International, Inc: RPTPα siRNA1, 5'-cggcagaaccagttaaaga-3'; RPTPα siRNA2, 5'-gcaccaacattcagcccaa-3'; RPTPα siRNA3, 5'-ggagaatggcagacgacaa-3'. The shRNA negative control, obtained from B-Bridge International, Inc. (Tokyo, Japan), has no homology to any human mRNA sequences in the NCBI Reference Sequence Database. We used pSH1-H1-H1-Puro shRNA Lentiviral Expression System (SBI Inc.) to generate lentivirus supernatants from HEK293FT cells. In brief, HEK293FT cells were seeded in 10-cm dishes at 5 X 106 cells/dish. After cells reached 90-95% confluence, the constructed shRNA expression vector (3 μg/dish) in ViraPower Packaging Mix (9 μg/dish) with Lipofectamine 2000 (Invitrogen Inc.) was transfected into HEK293FT cells. Twelve hours after initiating transfection, the plasmid-lipofectamine solution was removed, and the cell growth medium without antibiotics was added. The lentivirus-containing supernatants were harvested 48 and 72 h post-transfection. The AZ-521 cells were plated to 30-50% confluence and transfected with appropriate dilutions of lentivirus supernatants. 24 hours after transfection, the cells were cultured in cell growth medium containing Puromycin (0.5 μg/ml) to obtain the stable, transfected AZ-521 cells. After several selections, we isolated AZ-521 cells with knockdown of endogenous RPTPα.

Purification of VacA.

The toxin-producing *H. pylori* strain ATCC 49503 was the source of VacA for purification as previously described **(36)**.

Assay for vacuolating activity.

Vacuolating activity was assessed using AZ-521

cells as previously described **(36)**. Briefly, cells (1×10^4 cells/well, 100 μl) were grown as monolayers in 96-well culture plates for 24 h in a 5% CO_2 atmosphere at 37°C. VacA was added, and cells were incubated at 37°C for the indicated times. To quantify vacuolating activity, the uptake of neutral red into vacuoles was determined.

Preparation of Alexa555-labeled VacA.

To investigate VacA binding to cells and co-localization with other proteins in cells, VacA was labeled using the Alexa Fluor 555 Protein Labeling Kit (Molecular Probes), according to instructions provided by the manufacturer. In brief, 50 μl of 1 M sodium bicarbonate buffer (pH 8.5) were added to 500 μl (500 μg in phosphate-buffered saline (PBS)) of VacA, followed by incubation with the reactive dye in the vial for 15 min at room temperature. To remove excess dye, the reaction mixture was applied to a PD-10 column (Amersham Biosciences). Alexa 555-labed VacA (100 μg/ml) was stored at -20°C.

Purification and identification of p500

To purify p500 using affinity columns, AZ521 cells (5×10^7 cells) were washed twice with PBS, and suspended in 10 ml of Sol buffer containing 50 mM Tris-HCl, pH 7.5, 100 mM NaCl, 10% glycerol, 1% Triton X-100, with protease inhibitor cocktail [Roche diagnostic]) for 15 min on ice. After centrifugation (20 min, 17, 400 x g), the supernatant was filtered (0.45 μm, Millipore) and the filtrate (10 ml) applied to a Maackia amurensis (MAA)-agarose column (2 ml bed volume, Seikagaku Corporation). After washing the column, Sol buffer containing 50 mM ethylenediamine was used to elute the carbohydrate-containing proteins in 1 ml fractions. To confirm the presence of p500 in eluted fractions, proteins in effluents were detected by lectin blotting using MAA as described previously **(15,16)**. To identify p500, proteins in effluents were precipitated with chloroform/methanol, then heated at 100 ^oC for 10 min in 1x SDS-PAGE sample buffer, separated in 6% gels, and transferred to PVDF membranes, which were stained with CBB. The stained bands were used for LC-MS/MS analysis.

Immunoprecipitation

Immunoprecipitation of VacA-binding proteins from AZ521 cells was performed as described previously. In brief, biotinylated AZ521 cell lysates (100 μg/200 μl) were incubated at 4°C for 1 h with 1 μg of native VacA or heat-inactivated VacA (100°C, 10 min), followed by incubation at 4°C overnight with 1 μl of rabbit anti-VacA antibodies. Antibody-bound proteins were collected after addition of 20 μl of rProtein G Agarose (Invitrogen), 50% v/v in Sol buffer, and incubated at 4°C for 1.5 h. After beads were washed three times with Sol buffer, proteins were solubilized in SDS-PAGE sample buffer, resolved by SDS-PAGE, and transferred to PVDF membranes (Millipore; Immobilon-P membranes), which were incubated with streptavidin-HRP (Amersham Pharmacia Biotech). Biotinylated proteins were detected using the enhanced chemiluminescence system

(Pierce).

Immunofluorescence confocal microscopy

For immunofluorescence analysis of VacA co-localization with LRP1, RPTPα, RPTPβ or LC3B, AZ-521 cells (1×10^5 cells) on cover glass (Matsunami) were incubated with 120 nM Alexa555-labeled VacA for the indicated time, cells were fixed with 4% paraformaldehyde (PFA) at room temperature for 15 min, washed with PBS twice, and then immediately permeabilized with ice-cold 100% methanol for 10 minutes at -20^{o}C. The cells are then rinsed three times with PBS and incubated with blocking buffer (5% goat serum, 0.3% Triton X-100 in PBS) at room temperature for 1 h. To visualize LRP1 (8G1 antibody, 1:50), RPTPα (antibody provided by Jan Sap, 1:100), RPTPβ (polyclonal, 1:250) or LC3B (D11, 1:200), cells were further incubated with the primary antibodies in 1% BSA/ PBS buffer at 4°C overnight, washed twice with PBS and incubated with anti-rabbit Alexa488 (Molecular Probes), anti-mouse 488 (Molecular Probes), or anti-mouse Cy5 (Jackson ImmunResearch Laboratories.Inc) antibodies at room temperature for 1h in the dark. After washing with PBS three times, cells were mounted on glass slides using Prolong Gold Antifade reagent with DAPI. For staining the lysosomal compartment in VacA-treated cells, cells were incubated with 100 nM LysoTracker Red DND-99 (Molecular Probes) according to the instruction manual, before fixation with 4% PFA. Colocalization of VacA and the indicated proteins was analyzed by FV10i-LIV confocal microscopy (Olympus). The images were arranged with Adobe Photoshop CS4.

Statistics

Densitometric analysis on the immunoblots was done by Image Gauge software (FUJIFILM). The *p* values for densitometric analysis and vacuolating assay were determined by Student's *t* test with Graphpad Prism software (Graphpad, San Diego, CA). *p* values of <0.05 were considered statistically significant.

Results

Purification and identification of p500.

Our analysis of membrane proteins that bind VacA revealed three proteins, i.e., RPTP α, RPTP β, and an unidentified p500. The latter protein had a molecular mass higher than RPTPβ and reacted with MAA lectin **(15,16)**. In the present study, we purified p500 using MAA agarose-column chromatography and identified it by LC-MS/MS as low-density lipoprotein receptor-related protein 1 (LRP1) **(Fig. 1)**. We confirmed its association with native VacA by immunoprecipitation **(Fig. 1)**.

LRP1 mediates VacA binding and internalization in AZ-521 cells.

Confocal microscopy analysis revealed that in AZ-521 cells VacA colocalized with LRP1 on cell membranes, and was internalized, whereas heat-inactivated VacA did not show colocalization and internalization with LRP1 (data not shown) **(Fig. 2A)**. Furthermore, AZ-521 cells transfected with siRNA of LRP1 did not show significant toxin binding resulting in internalization, suggesting that LRP1

mediates VacA binding to the cell surface and facilitates its internalization. In agreement with these data, silencing of p500 gene inhibited vacuole formation caused by VacA **(Fig. 2B)**. These results suggest that LRP1 is associated with toxin internalization.

VacA induced generation of LC3-II in an LRP1-dependent manner.

Based on the prior reports **(28,29)** that VacA induced autophagy in AGS cells, we determined whether VacA induced LC3-II generation from LC3-I in AZ-521 cells. Consistent with previous findings, Western blot analysis showed that VacA induced LC3-II generation from LC3-I in a time-dependent manner (**Fig. 3a**). As expected, immunoblots of VacA-treated cells transfected with control siRNA indicated a progressive conversion over 10 h of LC3-I to LC3-II. In LRP1 siRNA-transfected cells, LRP1 expression was down-regulated after 4 h and conversion of LC3-II from LC3-I was suppressed (**Fig. 3b**). These data suggest an important role of LRP1 in mediating autophagy in AZ-521 cells in response to VacA.

VacA induced formation of autophagosomes and autolysosomes in AZ-521 cells.

To determine whether VacA induces autophagic vacuoles, AZ-521 cells were incubated with 120 nM VacA. We microscopically observed that active VacA (A) is sufficient to trigger autophagic vacuoles such as autophagosomes containing LC3-II after 4 h incubation, followed after 12 h incubation by formation of autolysosomes as detected by LysoTracker **(Fig. 4A)**. Cells incubated with heat-inactivated VacA (IA) showed low or undetectable levels of these autophagic vacuoles after 12 h incubation. Further, confocal microscopy analysis showed that intracellular VacA partially co-localized with LC3-II and LRP1, consistent with the conclusion that LRP1 plays an important role in VacA-induced autophagosome formation. However, LRP1 knockdown with siRNA suppressed VacA co-localization with LC3-II, suggesting that LRP1 is essential for formation of autophagosomes in response to VacA **(Fig. 4B).**

Vacuoles caused by VacA are characterized as autophagosomes and autophagolysosomes.

Confocal microscope visualization of LC3-II, VacA, and LRP1 revealed that vacuoles caused by VacA are of at least two different types; one type consists of autophagic vacuoles such as autophagosomes and autophagolysosomes and the second type lacks LC3-II **(Fig. 5A)**. These observations support the previous findings that VacA-dependent autophagosomes and large vacuoles are distinct intracellular compartments and autophagy is independent of the formation of large vacuoles by VacA **(29)**. Interestingly, some vacuoles observed with RPTPβ revealed small light vacuoles without LC3-II **(Fig. 5B)** and dense vacuoles with RPTPα were devoid of LC3-II **(Fig. 5C)**. Although little is known about the physiological importance of the autophagy-dependent degradation of mitochondria (mitophagy) **(39)**, several studies have suggested that PINK1/parkin-dependent mitophagy selectively degrades mitochondria

(40) , implying that mitophagy contributes to mitochondrial quality control. As shown in **Fig. 5D**, after 10 h-incubation mitochondria were not observed in vacuoles with LC3-II. Furthermore, recent studies revealed that p62 binds to LC3 on the autophagosome membrane to target aggregates to autophagosomes for degradation **(41)**. After 24 h incubation, VacA, not heat-inactivated VacA, induced formation of puncta, which were colocalized with LC3-II and p62 (**Fig. 5E and Supplementary Information, Fig. S1**).

Among VacA binding proteins, LRP1, but not RPTPs and FN, mediates VacA-dependent autophagy.

To assess which VacA-binding proteins were responsible for VacA-induced autophagy, we examined the effect of silencing and knock out of the genes for RPTPβ, RPTPα, and fibronectin. Although LRP1 silencing blocked VacA-stimulated generation of LC3-II as shown in Figure 3b, silencing these other genes did not show a similar effect, suggesting that only LRP1 may be critical for VacA-induced autophagy (**Fig. 6).**

LRP-1, but not RPTPs, mediates cleavage of caspase-7 and PARP caused by VacA.

Excessive autophagy can cause cell death **(34,42)** . Further, VacA-induced cell death may occur through a programmed necrosis pathway in a caspase-independent process in AZ-521 cells **(27)**. Therefore, we examined whether VacA-induced cell death resulted from autophagy via an LRP1-dependent pathway. Western blot analysis showed that LRP1 silencing blocked VacA-induced generation of LC3-II as well as cleavages of effector caspase-7 and PARP, suggesting that VacA binding to LRP-1 is responsible for not only autophagy but also for apoptosis in AZ-521 cells (**Fig. 7**).

Effects of Atg5 silencing, Z-VAD-FMK and Necrostatin-1 on VacA-induced LC3-II production and cleavage of PARP.

To further examine the link between autophagy and apoptosis, the effects of Atg5 silencing with siRNA, general caspase inhibitor (Z-VAD-FMK) and RIPK inhibitor (Necrostatin-1) on LC3-II generation and PARP cleavage was evaluated**.** Silencing of *Agt5* gene inhibited generation of LC3-II as well as PARP cleavages in response to VacA (**Fig. 8)**, whereas both inhibitors, Z-VAD-FMK and Necrostatin-1, which interferes with apoptosis **(43)**, did not inhibit VacA-induced autophagy, suggesting that VacA-induced autophagy precedes apoptosis in AZ-521 cells. Necrostatin-1, which inhibits necroptosis **(44)**, did not interfere with VacA-induced generation of LC3-II and PARP cleavage.

Effect of anion-channel blockers, NPPB and DIDS, on VacA-induced LC3-II production.

To assess whether membrane channels formed by VacA may also be involved in autophagy **(29)**, we tested the effects of pretreating AZ-521 or AGS cells with chloride channel blockers, NPPB and DIDS, which are known to block both VacA-mediated channel activity and

cellular vacuolation **(45)**. AZ-521 cells were pretreated for 30 min with 100 μM NPPB or 100 μM DIDS prior to incubation with VacA for 6 h. Both NPPB and DIDS inhibited VacA-induced LC3-II generation in AZ-521 cells (**Fig. 9a**), but not in AGS cells under these conditions (**Fig. 9b**).

Discussion

VacA has two functional domains, an N-terminal 33.4 kDa domain (named p33, p34 or p37, comprising residues 1-311) and a C-terminal domain of 54.8 kDa (named p55 or p58, comprising residues 312-821) **(10,46,47)**. Vacuolization of epithelial cells by VacA is strictly dependent on the formation of anion-selective membrane channels, which are targeted to late endosomes after internalization of the toxin **(45,48).** The pore and channel forming by N-terminal p33 domain alone drives pleiotropic cellular activities of VacA; i.e., vacuolation, mitochondria damage, apoptosis **(10,47)**, autophagy **(28,29)**, and programmed necrosis **(27)**, suggesting that VacA may be characterized as a pore-forming toxin **(47)**. Another study has indicated that both p33 and p55 are required to form a functional channel in the inner mitochondria membrane and trigger apoptosis **(49).** In addition, it is now widely accepted that the C-terminal p55 domain of VacA plays an essential role in its binding to target cells **(50,51)**.

The present study defines a novel role for VacA signaling through LRP1 in AZ-521 cells, inducing autophagy and apoptosis **(Fig. 7)**. LRP1 is a large endocytic receptor belonging to the LDL receptor family. This membrane protein consists of a 515-kDa heavy chain containing the extracellular ligand-binding domains and a non-covalently associated 85-kDa light chain, which consists of a transmembrane domain and a short cytoplasmic tail. LRP1 functions as a clearance receptor mediating the uptake and catabolism of various ligands from the pericellular environment, e.g., LRP1 binds to apolipoprotein E-rich lipoproteins, lipoprotein lipase, *α2*-macroglobulin, lactoferrin and tissue plasminogen activator; it functions in lipoprotein metabolism, degradation of proteases and proteinase/inhibitor complexes, activation of lysosomal enzymes and cellular entry of viruses and bacterial toxin such as *Pseudomonas* exotoxin A **(52)**. LRP1 has also been shown to function in the turnover of fibronectin **(53).**

This is the first study to provide evidence that LRP1 mediates autophagy. In AZ-521 cells, VacA triggered formation of autophagosomes, followed by autolysosome formation, consistent with the observations in AGS cells **(29).** Since LRP1 knockdown with siRNA resulted in inhibition of VacA-induced LC3-II generation and cleavage of both caspase 7 and PARP, induction by VacA of both autophagy and apoptosis occurred via, at least in part, association with LRP1. VacA also promoted formation of vacuoles containing RPTPβ and RPTPα, which were characterized as light and dense vacuoles respectively by confocal

microscopy, and large vacuoles **(Fig. 5)**. We observed the presence in AZ-521 cells of large vesicles without autophagosome markers in wild type and Atg12 knockdown AGS cells **(29)**. In generally, vacuole formation caused by VacA requires for VacA channel activity **(54).** Our studies using chloride channel blockers, NPPB and DIDS, to address the relationship between VacA-induced autophagy and channel activity of VacA in AZ-521 cells treated with VacA revealed that these channel blockers inhibited LC3-II generation response to VacA (**Fig. 9**), suggesting that channel activity may be required for LRP1-dependent autophagy. More interestingly, VacA-induced autophagy was not blocked by caspase inhibitor and RIPK inhibitor, suggesting that VacA-induced autophagy via LRP1 binding precedes apoptosis.

Autophagy is a degradation process that involves formation of autophagosomes, which engulf cytoplasmic components, and fuse with the lysosome/vacuole for degradation of contents. This process is considered cytoprotective but in certain settings excessive autophagy can cause cell death **(34,42)**. Little information exists concerning the molecular mechanisms underlying the regulation of apoptosis by autophagy. Our data indicate that autophagy induced by VacA does not involve the canonical pathway in which Beclin-1 initiates the generation of autophagosomes by forming a multiprotein complex with class III PI3K, because 3MA, a class III PI3K inhibitor, and silencing of Beclin-1 did not inhibit autophagy induced by VacA **(Supplementary Information, Fig. S2)**. The detailed mechanism by which VacA induces autophagy and apoptosis via LRP1 is not clear. Within VacA-intoxicated cells that provoke death signaling via mitochondrial damage, cells attempt to limit damage by seeking what catabolic benefits may be found in autophagy as indicated by Terebiznik et al. (2009). Therefore, once the stress-provoking, death-signaling response to VacA is overwhelming, autophagy is futile, and it is beneficial to induce apoptosis.

Future studies involving mouse models and human specimens will help to determine whether LRP1 plays a critical role in the pathobiology of *H. pylori* infection *in vivo*.

References

1. Wroblewski, L. E., Peek, R. M., Jr., and Wilson, K. T. (2010) *Clin Microbiol Rev* **23**, 713-739
2. Yamaoka, Y. (2010) *Nat Rev Gastroenterol Hepatol* **7**, 629-641
3. Telford, J. L., Ghiara, P., Dell'Orco, M., Comanducci, M., Burroni, D., Bugnoli, M., Tecce, M. F., Censini, S., Covacci, A., Xiang, Z., and et al. (1994) *J Exp Med* **179**, 1653-1658
4. Marchetti, M., Arico, B., Burroni, D., Figura, N., Rappuoli, R., and Ghiara, P. (1995) *Science* **267**, 1655-1658
5. Ghiara, P., Marchetti, M., Blaser, M. J., Tummuru, M. K., Cover, T. L., Segal, E. D.,

Tompkins, L. S., and Rappuoli, R. (1995) *Infect Immun* **63**, 4154-4160

6. Kuo, C. H., and Wang, W. C. (2003) *Biochem Biophys Res Commun* **303**, 640-644
7. Oldani, A., Cormont, M., Hofman, V., Chiozzi, V., Oregioni, O., Canonici, A., Sciullo, A., Sommi, P., Fabbri, A., Ricci, V., and Boquet, P. *Helicobacter pylori* counteracts the apoptotic action of its VacA toxin by injecting the CagA protein into gastric epithelial cells (2009) *PLoS Pathog* **5**, e1000603
8. Akada, J. K., Aoki, H., Torigoe, Y., Kitagawa, T., Kurazono, H., Hoshida, H., Nishikawa, J., Terai, S., Matsuzaki, M., Hirayama, T., Nakazawa, T., Akada, R., and Nakamura, K. (2010) *Dis Model Mech* **3**, 605-617
9. Kuck, D., Kolmerer, B., Iking-Konert, C., Krammer, P. H., Stremmel, W., and Rudi, J. (2001) *Infect Immun* **69**, 5080-5087
10. Cover, T. L., and Blanke, S. R. (2005) *Nat Rev Microbiol* **3**, 320-332
11. Yamasaki, E., Wada, A., Kumatori, A., Nakagawa, I., Funao, J., Nakayama, M., Hisatsune, J., Kimura, M., Moss, J., and Hirayama, T. (2006) *J Biol Chem* **281**, 11250-11259
12. Calore, F., Genisset, C., Casellato, A., Rossato, M., Codolo, G., Esposti, M. D., Scorrano, L., and de Bernard, M. (2010) *Cell Death Differ* **17**, 1707-1716
13. Jain, P., Luo, Z. Q., and Blanke, S. R. (2011) *Proc Natl Acad Sci U S A* **108**, 16032-16037
14. Papini, E., de Bernard, M., Milia, E., Bugnoli, M., Zerial, M., Rappuoli, R., and Montecucco, C. (1994) *Proc Natl Acad Sci U S A* **91**, 9720-9724
15. Yahiro, K., Niidome, T., Kimura, M., Hatakeyama, T., Aoyagi, H., Kurazono, H., Imagawa, K., Wada, A., Moss, J., and Hirayama, T. (1999) *J Biol Chem* **274**, 36693-36699
16. Yahiro, K., Wada, A., Nakayama, M., Kimura, T., Ogushi, K., Niidome, T., Aoyagi, H., Yoshino, K., Yonezawa, K., Moss, J., and Hirayama, T. (2003) *J Biol Chem* **278**, 19183-19189
17. Hennig, E. E., Godlewski, M. M., Butruk, E., and Ostrowski, J. (2005) *FEMS Immunol Med Microbiol* **44**, 143-150
18. Gupta, V. R., Patel, H. K., Kostolansky, S. S., Ballivian, R. A., Eichberg, J., and Blanke, S. R. (2008) *PLoS Pathog* **4**, e1000073
19. Papadimitriou, E., Mikelis, C., Lampropoulou, E., Koutsioumpa, M., Theochari, K., Tsirmoula, S., Theodoropoulou, C., Lamprou, M., Sfaelou, E., Vourtsis, D., and Boudouris, P. (2009) *Eur Cytokine Netw* **20**, 180-190
20. Fujikawa, A., Shirasaka, D., Yamamoto, S., Ota, H., Yahiro, K., Fukada, M., Shintani, T., Wada, A., Aoyama, N., Hirayama, T., Fukamachi, H., and Noda, M. (2003) *Nat Genet* **33**, 375-381
21. Gebert, B., Fischer, W., Weiss, E., Hoffmann, R., and Haas, R. (2003) *Science* **301**, 1099-1102
22. Boncristiano, M., Paccani, S. R., Barone, S., Ulivieri, C., Patrussi, L., Ilver, D., Amedei, A., D'Elios, M. M., Telford, J. L., and Baldari, C. T. (2003) *J Exp Med* **198**, 1887-1897

23. Sewald, X., Gebert-Vogl, B., Prassl, S., Barwig, I., Weiss, E., Fabbri, M., Osicka, R., Schiemann, M., Busch, D. H., Semmrich, M., Holzmann, B., Sebo, P., and Haas, R. Integrin subunit CD18 Is the T-lymphocyte receptor for the *Helicobacter pylori* vacuolating cytotoxin. (2008) *Cell Host Microbe* **3**, 20-29
24. Sewald, X., Jimenez-Soto, L., and Haas, R. PKC-dependent endocytosis of the *Helicobacter pylori* vacuolating cytotoxin in primary T lymphocytes (2011) *Cell Microbiol* **13**, 482-496
25. Cover, T. L., Krishna, U. S., Israel, D. A., and Peek, R. M., Jr. (2003) *Cancer Res* **63**, 951-957
26. Singh, M., Prasad, K. N., Saxena, A., and Yachha, S. K. (2006) *Curr Microbiol* **52**, 254-260
27. Radin, J. N., Gonzalez-Rivera, C., Ivie, S. E., McClain, M. S., and Cover, T. L. *Helicobacter pylori* VacA induces programmed necrosis in gastric epithelial cells (2011) *Infect Immun* **79**, 2535-2543
28. Raju, D., Hussey, S., Ang, M., Terebiznik, M. R., Sibony, M., Galindo-Mata, E., Gupta, V., Blanke, S. R., Delgado, A., Romero-Gallo, J., Ramjeet, M. S., Mascarenhas, H., Peek, R. M., Correa, P., Streutker, C., Hold, G., Kunstmann, E., Yoshimori, T., Silverberg, M. S., Girardin, S. E., Philpott, D. J., El Omar, E., and Jones, N. L. (2012) *Gastroenterology* **142**, 1160-1171
29. Terebiznik, M. R., Raju, D., Vazquez, C. L., Torbricki, K., Kulkarni, R., Blanke, S. R., Yoshimori, T., Colombo, M. I., and Jones, N. L. (2009) *Autophagy* **5**, 370-379
30. Lum, J. J., Bauer, D. E., Kong, M., Harris, M. H., Li, C., Lindsten, T., and Thompson, C. B. (2005) *Cell* **120**, 237-248
31. Gozuacik, D., and Kimchi, A. (2004) *Oncogene* **23**, 2891-2906
32. McPhee, C. K., Logan, M. A., Freeman, M. R., and Baehrecke, E. H. (2010) *Nature* **465**, 1093-1096
33. Wirawan, E., Vande Walle, L., Kersse, K., Cornelis, S., Claerhout, S., Vanoverberghe, I., Roelandt, R., De Rycke, R., Verspurten, J., Declercq, W., Agostinis, P., Vanden Berghe, T., Lippens, S., and Vandenabeele, P. Caspase-mediated cleavage of Beclin-1 inactivates Beclin-1-induced autophagy and enhances apoptosis by promoting the release of proapoptotic factors from mitochondria (2010) *Cell Death Dis* **1**, e18
34. Maiuri, M. C., Criollo, A., and Kroemer, G. (2010) *EMBO J* **29**, 515-516
35. Rubinstein, A. D., Eisenstein, M., Ber, Y., Bialik, S., and Kimchi, A. (2011) *Mol Cell* **44**, 698-709
36. Nakayama, M., Hisatsune, J., Yamasaki, E., Nishi, Y., Wada, A., Kurazono, H., Sap, J., Yahiro, K., Moss, J., and Hirayama, T. (2006) *Infect Immun* **74**, 6571-6580
37. Hoyer-Hansen, M., Bastholm, L., Mathiasen, I. S., Elling, F., and Jaattela, M. (2005) *Cell Death Differ* **12**, 1297-1309
38. Yang, S., Wang, X., Contino, G., Liesa, M., Sahin, E., Ying, H., Bause, A., Li, Y., Stommel, J. M., Dell'antonio, G., Mautner, J., Tonon, G., Haigis, M., Shirihai, O. S., Doglioni, C.,

Bardeesy, N., and Kimmelman, A. C. (2011) *Genes Dev* **25**, 717-729
39. Youle, R. J., and Narendra, D. P. (2011) *Nat Rev Mol Cell Biol* **12**, 9-14
40. Vives-Bauza, C., and Przedborski, S. (2011) *Trends Mol Med* **17**, 158-165
41. Kirkin, V., McEwan, D. G., Novak, I., and Dikic, I. (2009) *Mol Cell* **34**, 259-269
42. Yoshimori, T. (2007) *Cell* **128**, 833-836
43. Zhu, H., Fearnhead, H. O., and Cohen, G. M. (1995) *FEBS Lett* **374**, 303-308
44. Degterev, A., Huang, Z., Boyce, M., Li, Y., Jagtap, P., Mizushima, N., Cuny, G. D., Mitchison, T. J., Moskowitz, M. A., and Yuan, J. (2005) *Nat Chem Biol* **1**, 112-119
45. Tombola, F., Carlesso, C., Szabo, I., de Bernard, M., Reyrat, J. M., Telford, J. L., Rappuoli, R., Montecucco, C., Papini, E., and Zoratti, M. (1999) *Biophys J* **76**, 1401-1409
46. Montecucco, C., and Rappuoli, R. (2001) *Nat Rev Mol Cell Biol* **2**, 457-466
47. Boquet, P., and Ricci, V. Intoxication strategy of *Helicobacter pylori* VacA toxin (2012) *Trends Microbiol* **20**, 165-174
48. Szabo, I., Brutsche, S., Tombola, F., Moschioni, M., Satin, B., Telford, J. L., Rappuoli, R., Montecucco, C., Papini, E., and Zoratti, M. (1999) *EMBO J* **18**, 5517-5527
49. Foo, J. H., Culvenor, J. G., Ferrero, R. L., Kwok, T., Lithgow, T., and Gabriel, K. (2010) *J Mol Biol* **401**, 792-798
50. Torres, V. J., Ivie, S. E., McClain, M. S., and Cover, T. L. (2005) *J Biol Chem* **280**, 21107-21114
51. Isomoto, H., Moss, J., and Hirayama, T. (2010) *Tohoku J Exp Med* **220**, 3-14
52. Herz, J., and Strickland, D. K. (2001) *J Clin Invest* **108**, 779-784
53. Salicioni, A. M., Gaultier, A., Brownlee, C., Cheezum, M. K., and Gonias, S. L. (2004) *J Biol Chem* **279**, 10005-10012
54. Genisset, C., Puhar, A., Calore, F., de Bernard, M., Dell'Antone, P., and Montecucco, C. The concerted action of the *Helicobacter pylori* cytotoxin VacA and of the v-ATPase proton pump induces swelling of isolated endosomes (2007) *Cell Microbiol* **9**, 1481-1490

Footnotes

We thank K. Maeda for skillful assistance and P.I. Padilla (University of the Philippines Visayas, Philippines) and B De Guzman (St. Luke's Medical Center, Philippines) for helpful discussions. This work was supported by Grants-in-Aid for Scientific Research from the Ministry of Education, Culture, Sports, Science and Technology of Japan and Improvement of Research Environment for Young Researchers from the Japan Science and Technology Agency. J.M. was supported by the Intramural Research Program, National Institutes of Health, National Heart, Lung, and Blood Institute.

Figure legends

Figure 1. Purification of p500 from AZ-521 cells by MAA-agarose column.

a. After biotinylation of surface proteins, AZ-521 cells were solubilized and immunoprecipitated with heat-inactivated (IA) or wild-type VacA (A) as described in Materials and Methods. Immunocomplexes were separated by SDS-PAGE in 6 % gels and transferred to PVDF membranes. VacA-binding proteins were detected with streptavidin-HRP.

b. Proteins immunoprecipitated with heat-inactivated (IA) or wild-type VacA (A) were separated by SDS-PAGE in 6 % gels and transferred to PVDF membranes, which were incubated with MAA-lectin conjugated to digoxigenin and then with anti-digoxigenin Fab fragments conjugated to alkaline phosphatase, followed by reaction with 4-nitro blue tetrazolium chloride/5-bromo-4-chloro-3-indolyl phosphate.

c. Biotinylated AZ-521 cell lysates were incubated overnight with a MAA-agarose column (2 ml bed volume), which was washed with 20 ml of Sol buffer. Bound proteins were eluted, concentrated and separated by SDS-PAGE as described in Materials and Methods. MAA-lectin blotting is shown in the left panel and CBB staining in the right panel. The stained p500 protein band was hydrolyzed with trypsin and subjected to LC-MS/MS analysis. The procedures described in Figure 1a-c were repeated at least three times with similar results.

Figure 2. LRP1-dependent VacA internalization and vacuolation in AZ-521 cells.

a. Confocal microscopic analysis of VacA binding to AZ-521 cells via LRP1. Non-targeting (NC) or LRP1 siRNA-transfected AZ-521 cells were incubated with Alexa555-labeled VacA (red) for 30 min at 4 ^{o}C or for 1 h at 37 ^{o}C, fixed with 4% paraformaldehyde and reacted with anti-LRP1 antibodies (green) as described in Materials and Methods. The nuclei were stained with DAPI. A merged picture shows co-localization of VacA and LRP1 in AZ-521 cells. Bars represent 20 μm. Experiments were repeated two times with similar results.

b. Silencing of LRP1 gene inhibited VacA-induced vacuolation. The indicated siRNA-transfected AZ-521 cells were incubated with 120 nM heat-inactivated (IA) or wild-type VacA (A) for 18 h at 37 ^{o}C. Vacuolating activity was evaluated by neutral red uptake assay as described in Materials and Methods. Data are presented as mean ±SD and significance is **P*<0.01 (n=3). Experiments were repeated three times with similar results.

Figure 3. VacA induced generation of LC3-II in an LRP1-dependent manner.

a. AZ-521 cells were incubated with 120 nM heat-inactivated (IA) or wild-type VacA (A) for the indicated time points and harvested for immunoblotting with the indicated antibodies. Quantification of VacA-induced LC3-II levels in AZ-521 cells was performed by densitometry

(bottom panel). Data are presented as mean ±SD of values from two experiments. Experiments were repeated two times with similar results.

b. The indicated siRNA-transfected AZ-521 cells were incubated with 120 nM heat-inactivated (IA) or wild-type VacA (A) for 4-5 h at 37 °C and the cell lysates were subjected to immunoblotting with the indicated antibodies. α-Tubulin served as a loading control. Quantification of VacA-induced LC3-II levels in AZ-521 cells was performed by densitometry (bottom panel). Data are presented as mean ±SD and significance is **P*<0.01 (n=4). Experiments were repeated four times with similar results.

Figure 4. VacA induced formation of autophagic vacuoles in AZ-521 cells via LRP1.

a. VacA-induced formation of autophagosomes and autolysosomes in AZ-521 cells.
AZ-521 cells were incubated with 120 nM heat-inactivated (IA) or wild-type VacA (A) for indicated time points and fixed for immunofluorescence staining with LC3B (green) antibodies as described in Materials and Methods. The acidic autophagolysosomes were stained by LysoTracker, as described in Materials and Methods. A merged picture shows co-localization in AZ-521 cells. The nuclei were stained with DAPI. Bars represent 20 μm. Experiments were repeated two times with similar results.

b. Induction of autophagy by VacA in an LRP1-dependent manner.
The indicated siRNA-transfected AZ-521 cells were incubated with 120 nM Alexa555-labed VacA (red) for 10 h at 37 °C and fixed for immunofluorescence staining with anti-LC3B (green) or anti-LRP1 (blue) antibodies as described in Materials and Methods. A merged picture shows co-localization in AZ-521 cells. The nuclei were stained with DAPI. Bars represent 20 μm. Experiments were repeated two times with similar results.

Figure 5. Various vacuoles formed by VacA.

a. Small autophagic vacuoles induced by VacA contain LC3-II, LRP1 and toxin: AZ-521 cells were incubated with 120 nM Alexa555-labed VacA (red) for 10 h at 37 °C and fixed for immunofluorescence staining with anti-LC3B (green), or anti-LRP1 (blue) antibodies or the nuclei were stained with DAPI as described in Materials and Methods. A merged picture shows co-localization in AZ-521 cells. Solid arrows show VacA, LC3B and LRP1 colocalization to puncta. Bars represent 20 μm. Experiments were repeated two times with similar results.

b. VacA-induced light vacuoles contain toxin and RPTPβ, and are different from autophagic vacuoles: AZ-521 cells were treated with 120 nM Alexa555-labed VacA (red) as similar to above.

Cells were fixed and stained for anti-LC3B (blue), anti-RPTPβ (green) and with DAPI. A merged picture shows co-localization in AZ-521 cells. Solid arrows show VacA and RPTPβ colocalization to puncta. Bars represent 20 μm. Experiments were repeated two times with similar results.

c. VacA-induced dense vacuoles contain toxin and RPTPα, and are different from autophagic vacuoles: AZ-521 cells were treated with 120 nM Alexa555-labed VacA (red) as similar to above. Cells were fixed and stained for anti-LC3B (blue), anti-RPTPα (green) and with DAPI. A merged picture shows co-localization in AZ-521 cells. Solid arrows show VacA and RPTPα colocalization to puncta. Bars represent 20 μm. Experiments were repeated two times with similar results.

d. VacA-induced autophagic vacuoles do not contain functional mitochondria: AZ-521 cells were treated with 120 nM heat-inactivated (IA) or native VacA (A) for 10 h at 37 ^{o}C and 100 nM MitoTracker (red) added to cells before fixation as described in Materials and Methods. Cells were stained for anti-LC3B (green), anti-p62 (green) and with DAPI. Bars represent 20 μm. Experiments were repeated two times with similar results.

e. VacA induced p62 generation in a time-dependent manner. AZ-521 cells were treated with 120 nM heat-inactivated (IA) or native VacA (A) for the indicated time points at 37 ^{o}C. Cells were fixed and stained for anti-LC3B (red) and with DAPI. Merged and higher magnification images of the outlined areas are shown. Bars represent 20 μm. Experiments were repeated two times with similar results.

Figure 6. Among VacA-binding proteins, LRP1, but not RPTPs and FN, mediates VacA-dependent autophagy.

a. The indicated siRNA-transfected AZ-521 cells were incubated with 120 nM heat-inactivated (IA) or wild-type VacA (A) for 4-5 h at 37 ^{o}C and the cell lysates were subjected to immunoblotting with the indicated antibodies. The knockdown levels of RPTPβ or RPTPα were detected by the antibodies (right panel). α-Tubulin served as a loading control.

b. The indicated NC or RPTPβ siRNA transfected AZ-521 cells were incubated with 120 nM heat-inactivated (IA) or wild-type VacA (A) for 4-5 h at 37 ^{o}C and the cell lysates were subjected to immunoblotting with anti-LC3B or anti-fibronectin (FN) antibodies. α-Tubulin served as a loading control.

c. AZ-521 cells were transfected with NC or fibronectin (FN) siRNA and treated with heat-inactivated (IA) or wild-type VacA (A) for 4-5 h at 37 ^{o}C. Cell lysates were subjected to immunoblotting with the indicated antibodies. α-Tubulin served as a loading control. A blot representative of at least three separate experiments is shown.

Figure 7. LRP1, but not RPTPs, mediates VacA-dependent cleavage of caspase -7 and PARP.

a. NC or LRP1 siRNA-transfected AZ-521 cells were incubated with 120 nM heat-inactivated (IA) or wild-type VacA (A) for 6 h at 37 ^{o}C and the cell lysates were subjected to immunoblotting with anti-LC3B, anti-cleaved PARP, anti-cleaved caspase-7, or anti-LRP1 antibodies. α-Tubulin served as a loading control. A blot representative of four separate experiments is shown. Quantification of VacA-induced cleavage of PARP (cPARP) or caspase-7 (cCas7) levels in the indicated siRNA-transfected AZ-521 cells was performed by densitometry (bottom panel). Data are presented as mean ±SD and significance is **P*<0.01 (n=4) and ***P*<0.03 (n=4).

b. The indicated siRNA-transfected AZ-521 cells were incubated with 120 nM heat-inactivated (IA) or wild-type VacA (A) for 6 h at 37 ^{o}C and the cell lysates were subjected to immunoblotting with anti-LC3B, anti-cleaved PARP, anti-RPTPα, or anti-RPTPβ antibodies. α-Tubulin served as a loading control. A blot representative of three separate experiments is shown.

Figure 8. Effects of Atg5 silencing, Z-VAD-FMK, and Necrostatin-1 on VacA-induced LC3-II generation and PARP cleavage.

a. The indicated siRNA-transfected AZ-521 cells were incubated with 120 nM heat-inactivated (IA) or wild-type VacA (A) for 8-10 h at 37 ^{o}C and the cell lysates were subjected to immunoblotting with anti-LC3B, anti-cleaved PARP or anti-Atg5 antibodies. α-Tubulin, as a loading control. A blot representative of three separate experiments is shown. Quantification of VacA-induced LC3-II or PARP cleavage (cPARP) in the indicated siRNA-transfected AZ-521 cells was performed by densitometry (bottom panel). Data are presented as mean ±SD and significance is **P*<0.05 (n=5) and ***P*<0.01(n=5).

b. AZ-521 cells were pretreated with 50 μM Z-VAD-FMK (Z-VAD) or 50 μM Necrostatin-1 (Necrostatin) for 30 min, and then 120 nM heat-inactivated (IA) or wild-type VacA (A) were added to cells. After 10 h of incubation at 37°C, cell lysates were analyzed by Western blotting using antibodies against LC3B and cleaved PARP. α-Tubulin served as a loading control. Data are representative of three separate experiments. Quantification of VacA-induced PARP cleavage (cPARP) levels in the indicated siRNA-transfected AZ-521 cells was performed by densitometry (bottom panel). Data are presented as mean ±SD and significance is **P*<0.01 (n=3)

Figure 9. Effect of anion-channel inhibitor on VacA-induced LC3-II generation.

AZ-521 (**a**) or AGS (**b**) cells were pretreated with 100 μM NPPB or DIDS for 30 min at 37 ^{o}C and then incubated with 120 nM heat-inactivated (IA) or wild-type VacA (A) for 4 h at 37 ^{o}C. Cell lysates were subjected to immunoblotting with anti-LC3B antibody or anti-α-Tubulin

antibody as a loading control. Quantification of VacA-induced LC3-II levels in the cells was performed by densitometry (bottom panel). Data are means and SD of values from two independent experiments.

Fig. 1

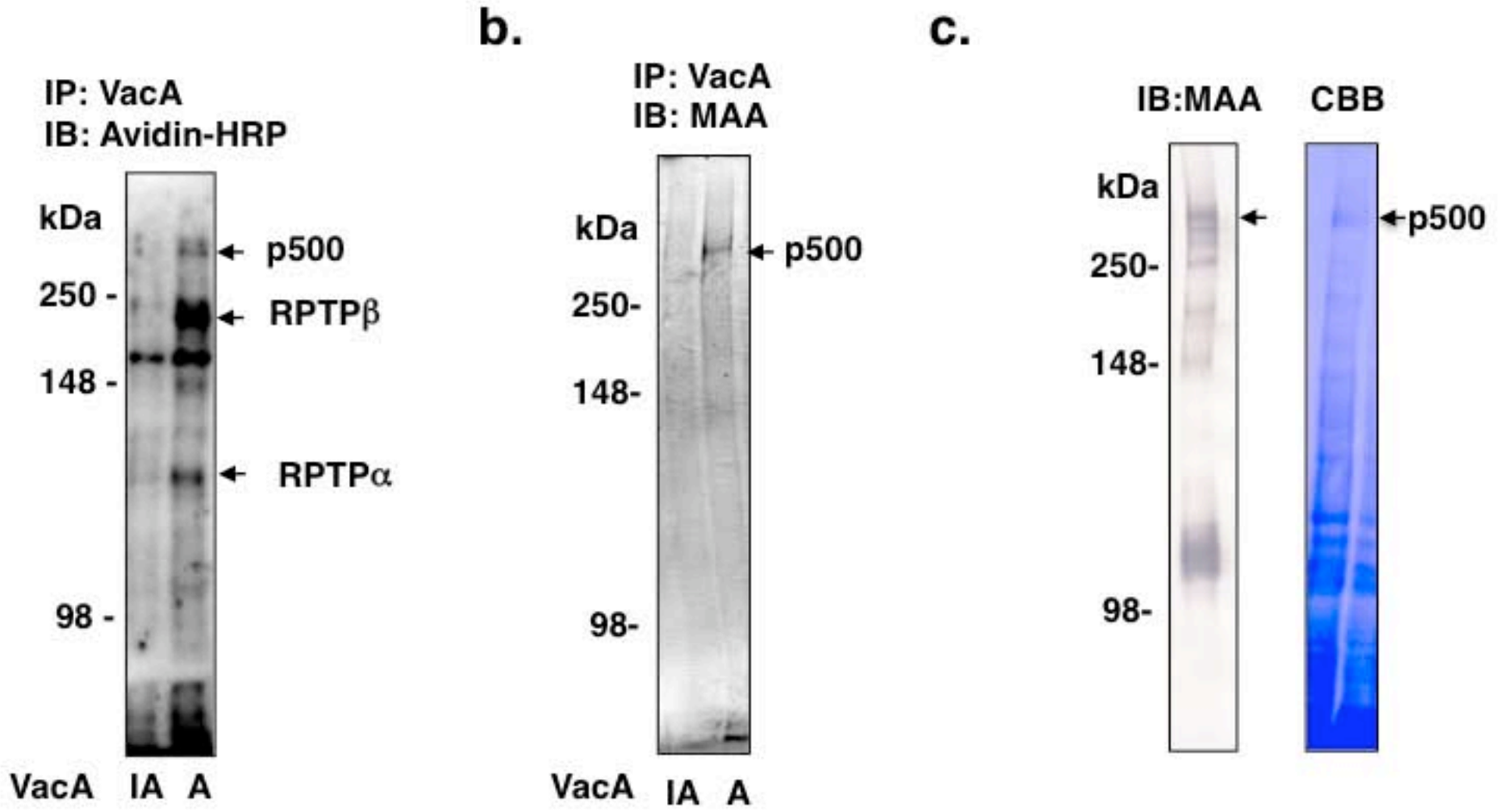
a.
IP: VacA
IB: Avidin-HRP
kDa
250 -
148 -
98 -
p500
RPTPβ
RPTPα
VacA IA A
b.
IP: VacA
IB: MAA
kDa
250-
148-
98-
p500
VacA IA A
c.
IB:MAA
CBB
kDa
250-
148-
98-
p500

Fig. 2A

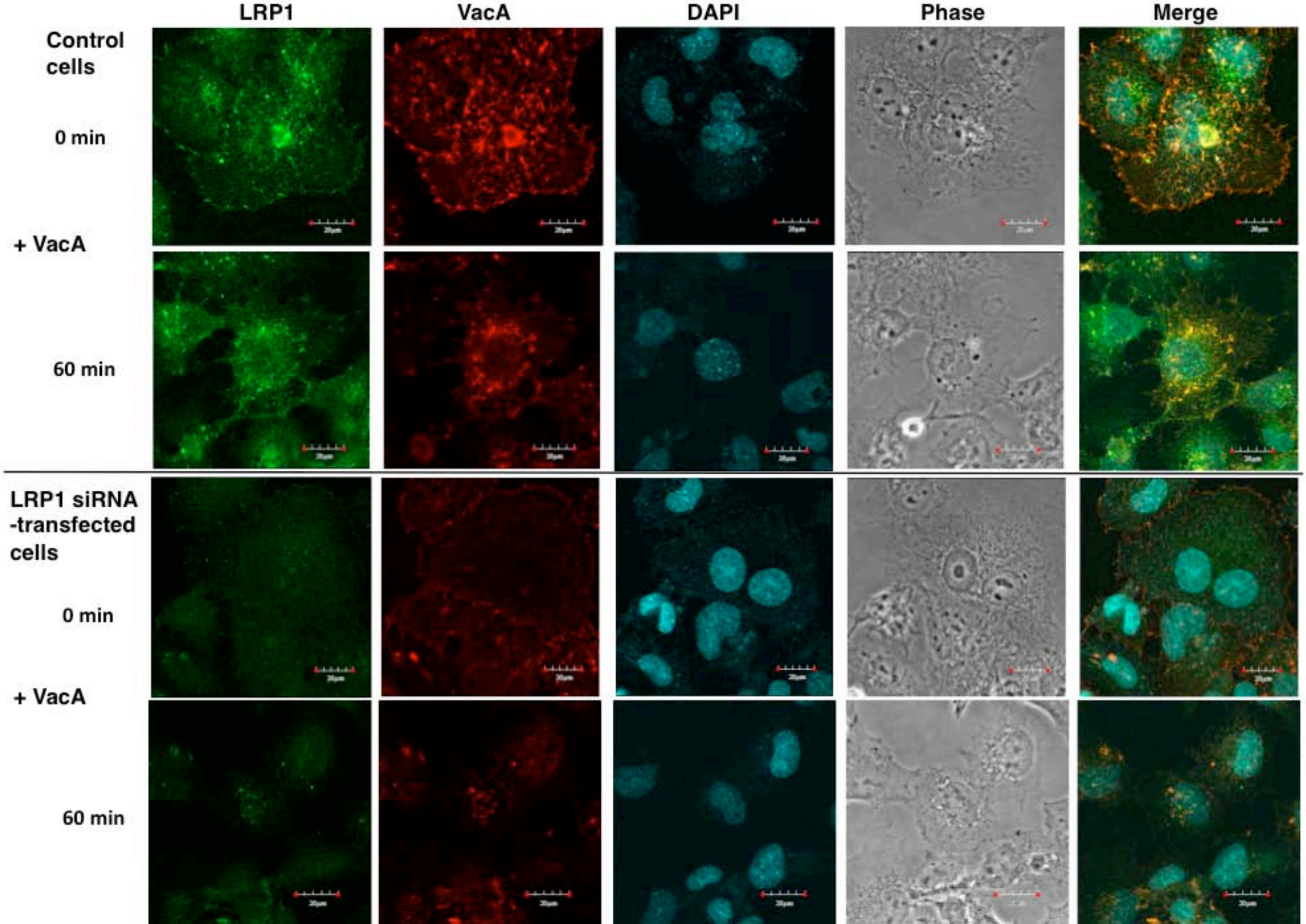
LRP1
VacA
DAPI
Phase
Merge
Control cells
0 min
+ VacA
60 min
LRP1 siRNA -transfected cells
0 min
+ VacA
60 min

Fig. 2B

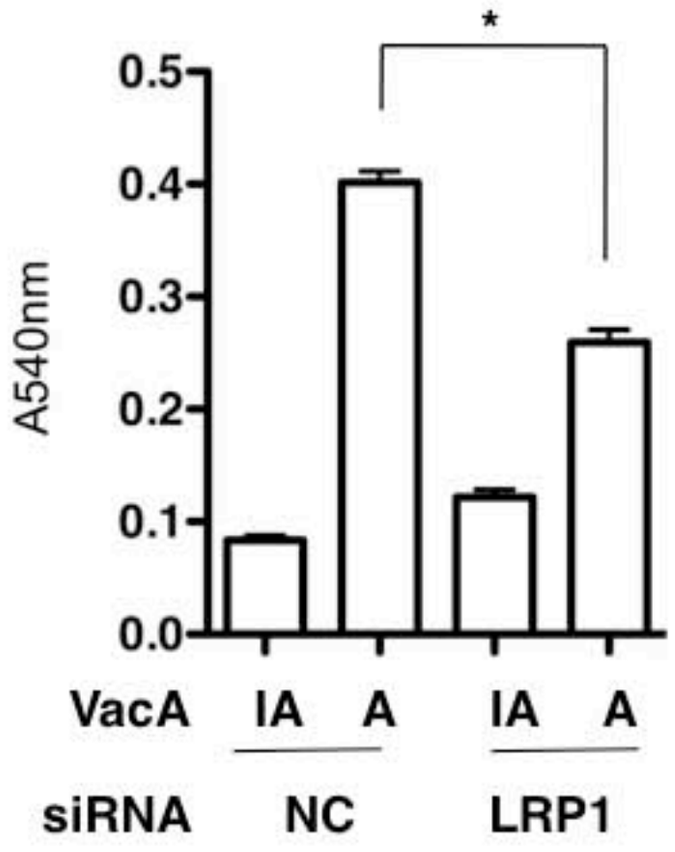

Fig. 3

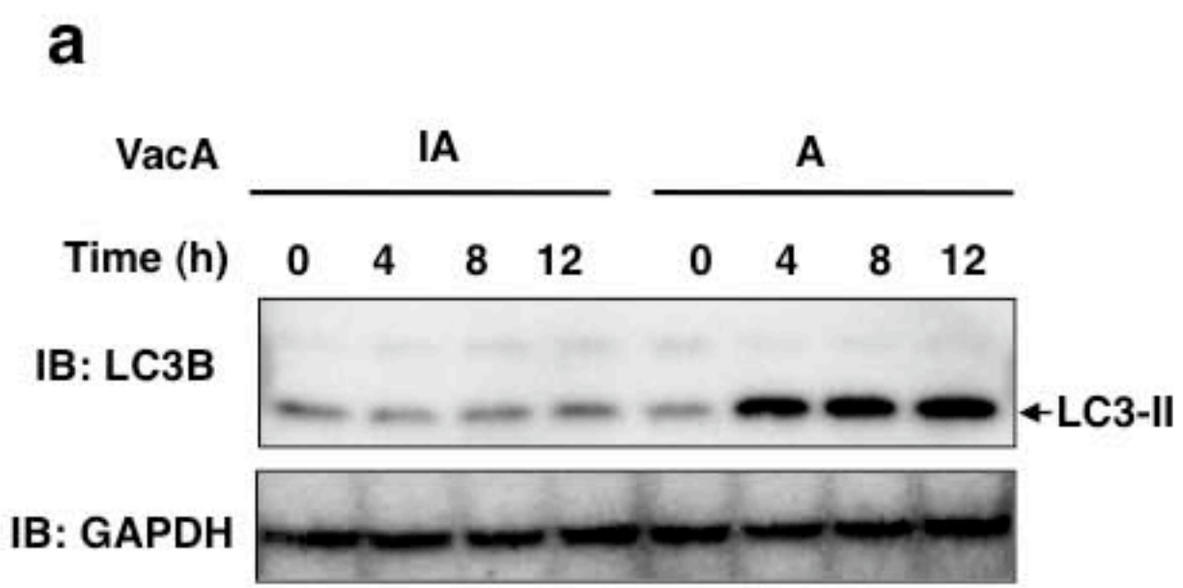
a
VacA
IA
A
Time (h)
0 4 8 12 0 4 8 12
IB: LC3B
LC3-II
IB: GAPDH
LC3B-II/GAPDH (fold increase)
0 1 2 3 4
Time (h)
0 4 8 12 0 4 8 12
VacA
IA
A

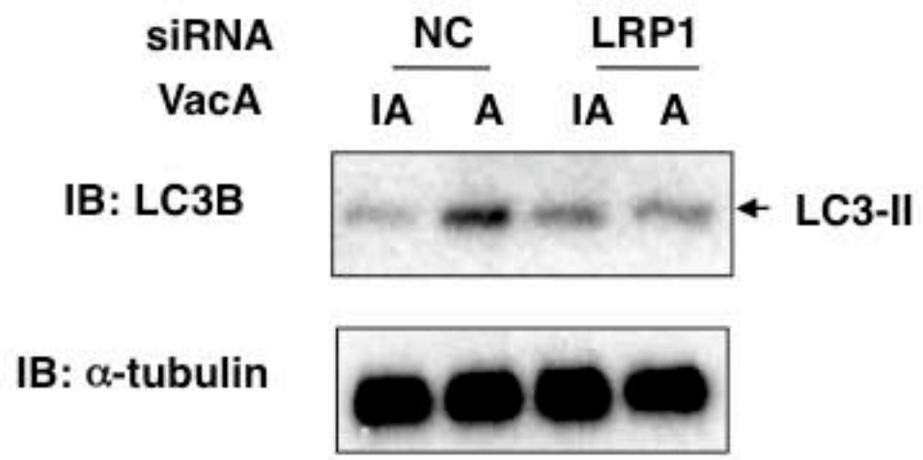
b
siRNA
NC
LRP1
VacA
IA A IA A
IB: LC3B
LC3-II
IB: α-tubulin
siRNA
NC LRP1
IB: LRP1
LC3B-II/tubulin (fold increase)
0 2 4 6 8
*
VacA
IA A IA A
siRNA
NC
LRP1

Fig. 4A

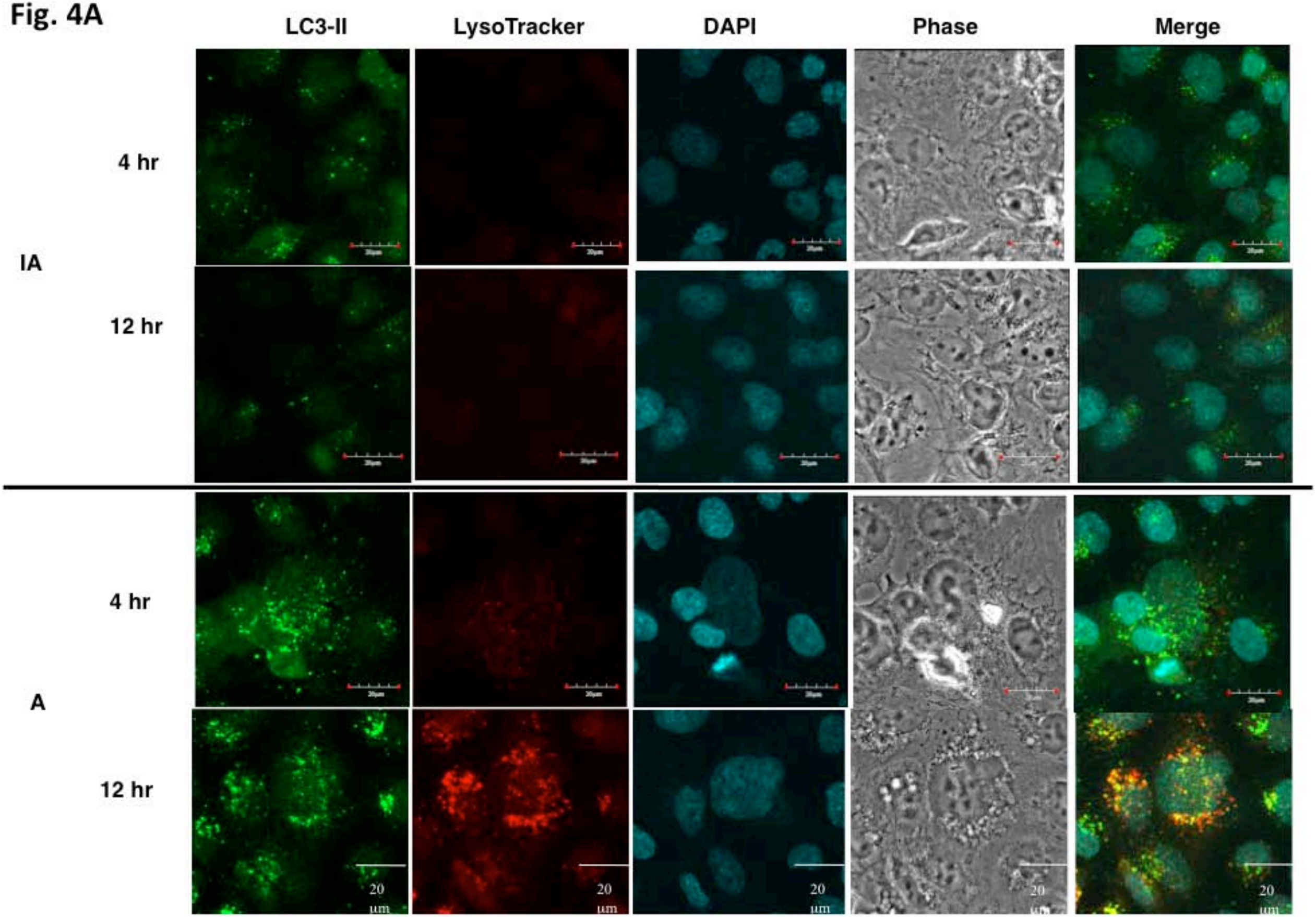
LC3-II
LysoTracker
DAPI
Phase
Merge
IA
4 hr
12 hr
A
4 hr
12 hr
20 um
20 um
20 um
20 um
20 um

Fig. 4B

VacA
10h incubation

NC siRNA
transfection

LC3-II

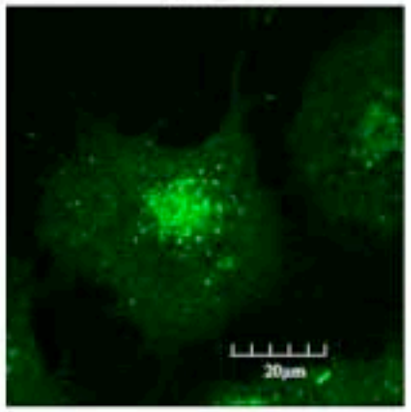

Alexa555-VacA

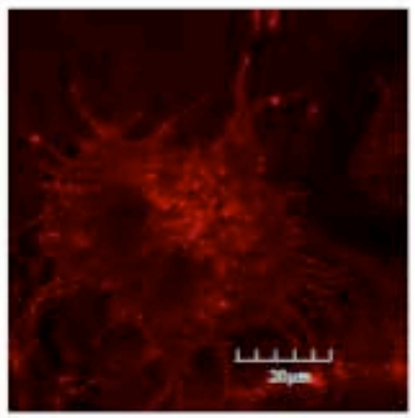

DAPI

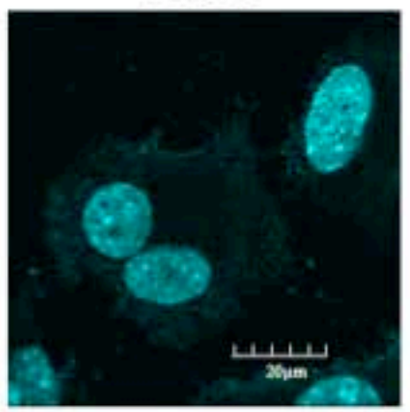

LRP1

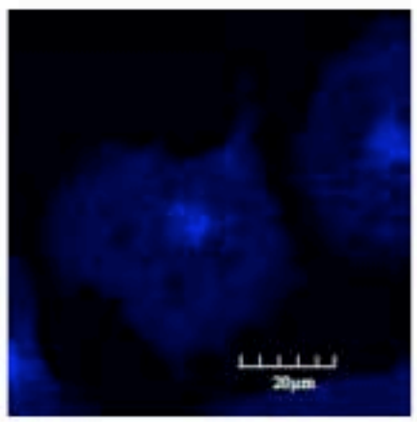

Phase

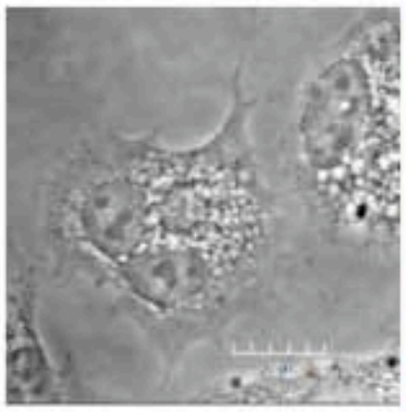

Merge(LC3-II/VacA/DAPI)

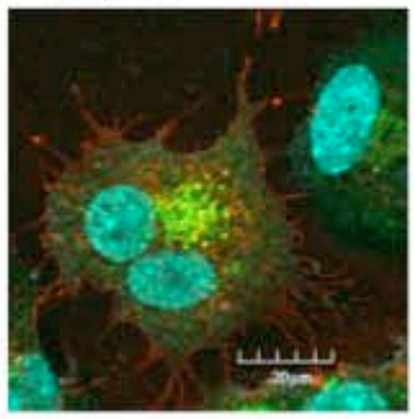

Merge

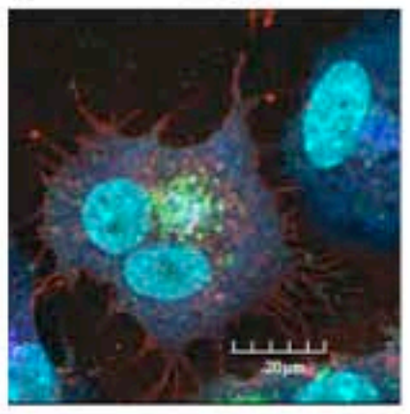

LRP1 siRNA
transfection

LC3-II

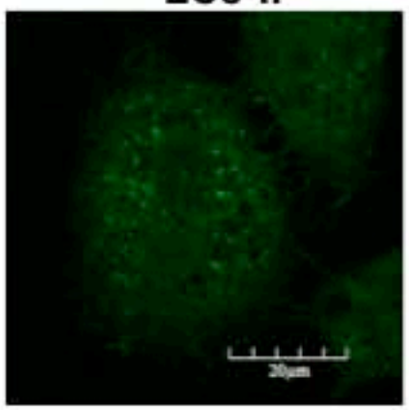

Alexa555-VacA

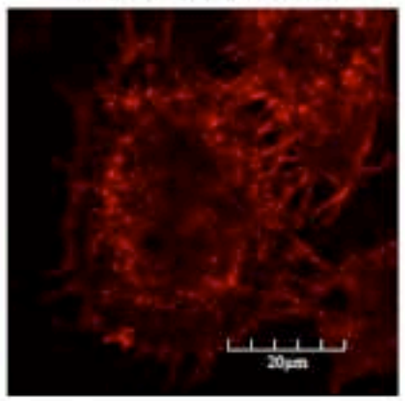

DAPI

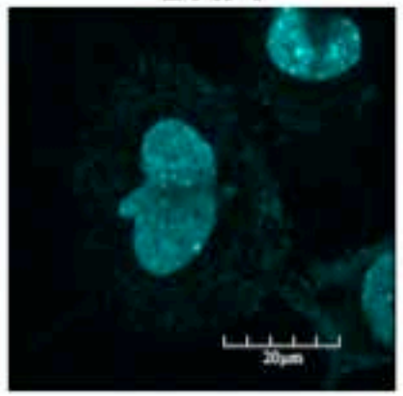

LRP1

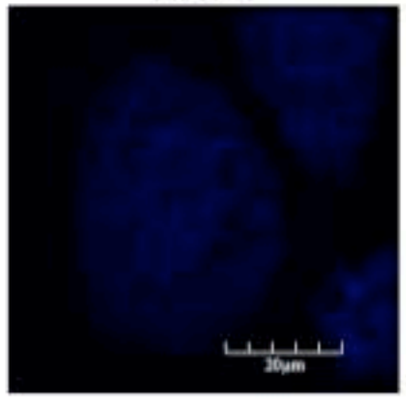

Phase

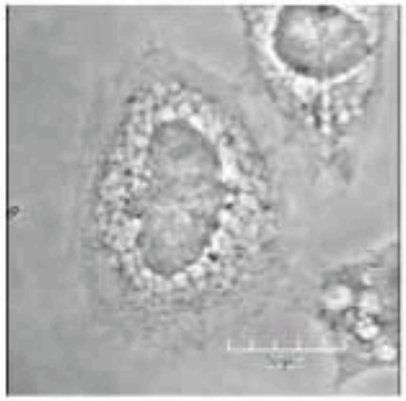

Merge(LC3-II/VacA/DAPI)

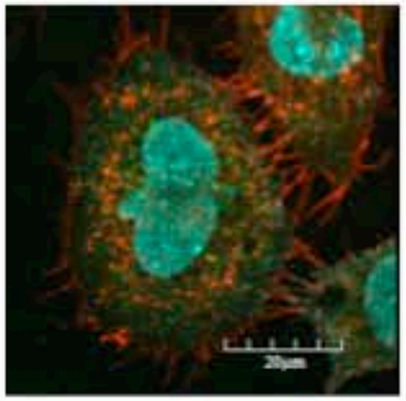

Merge

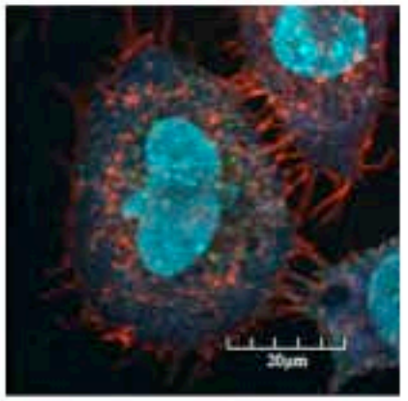

Fig. 5A

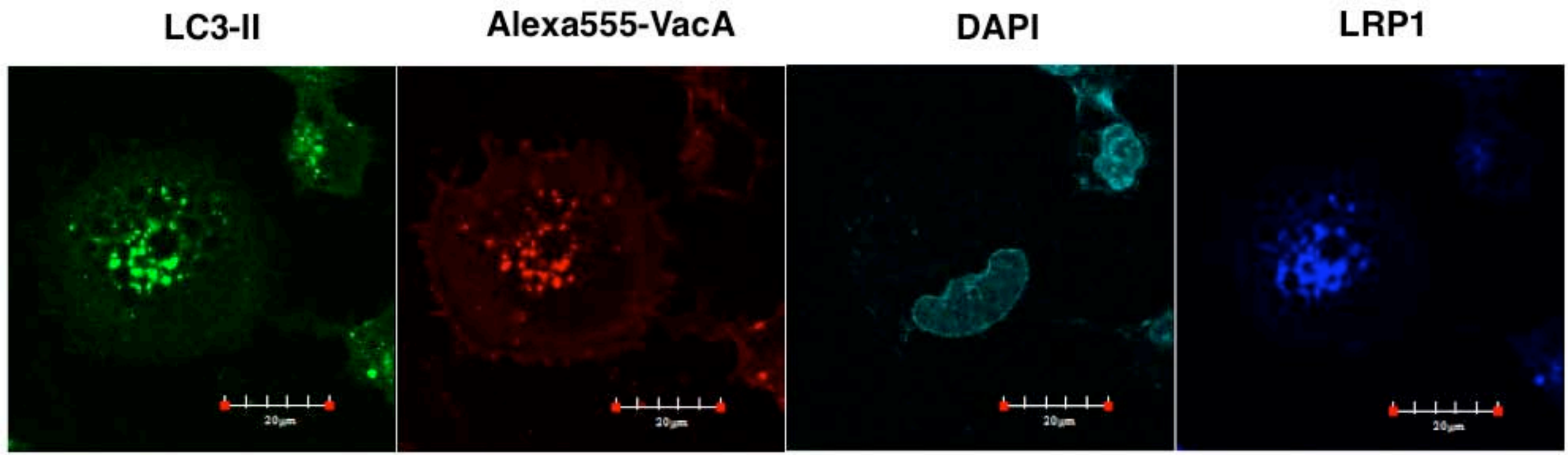

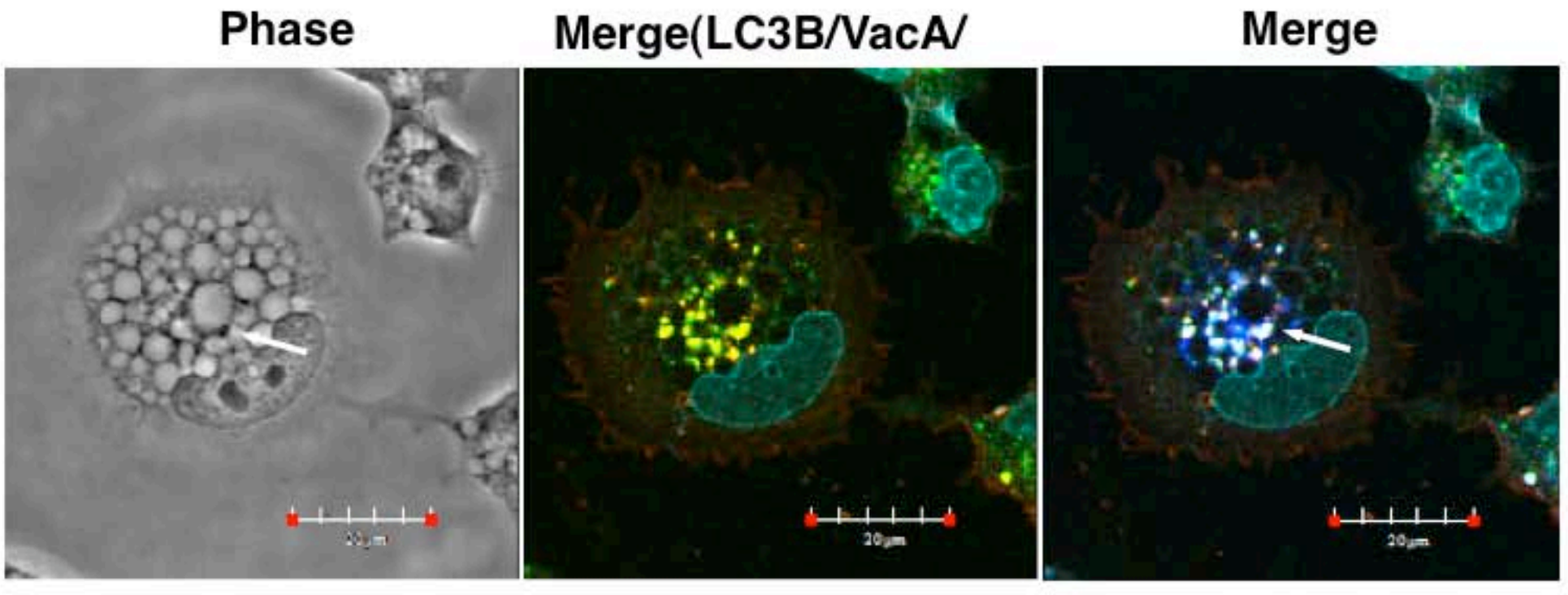

Fig. 5B

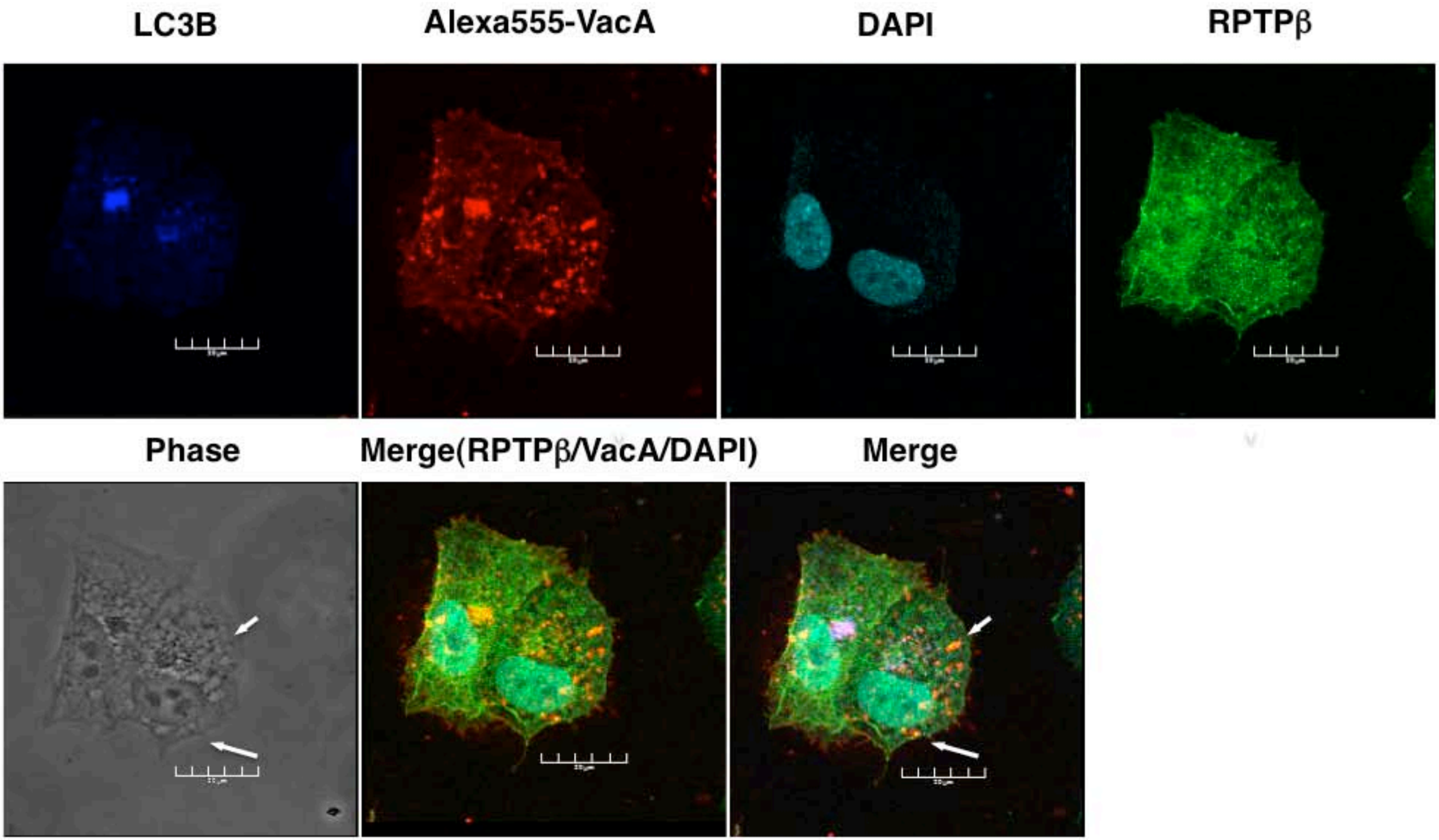
LC3B
Alexa555-VacA
DAPI
RPTPβ
Phase
Merge(RPTPβ/VacA/DAPI)
Merge

Fig. 5C

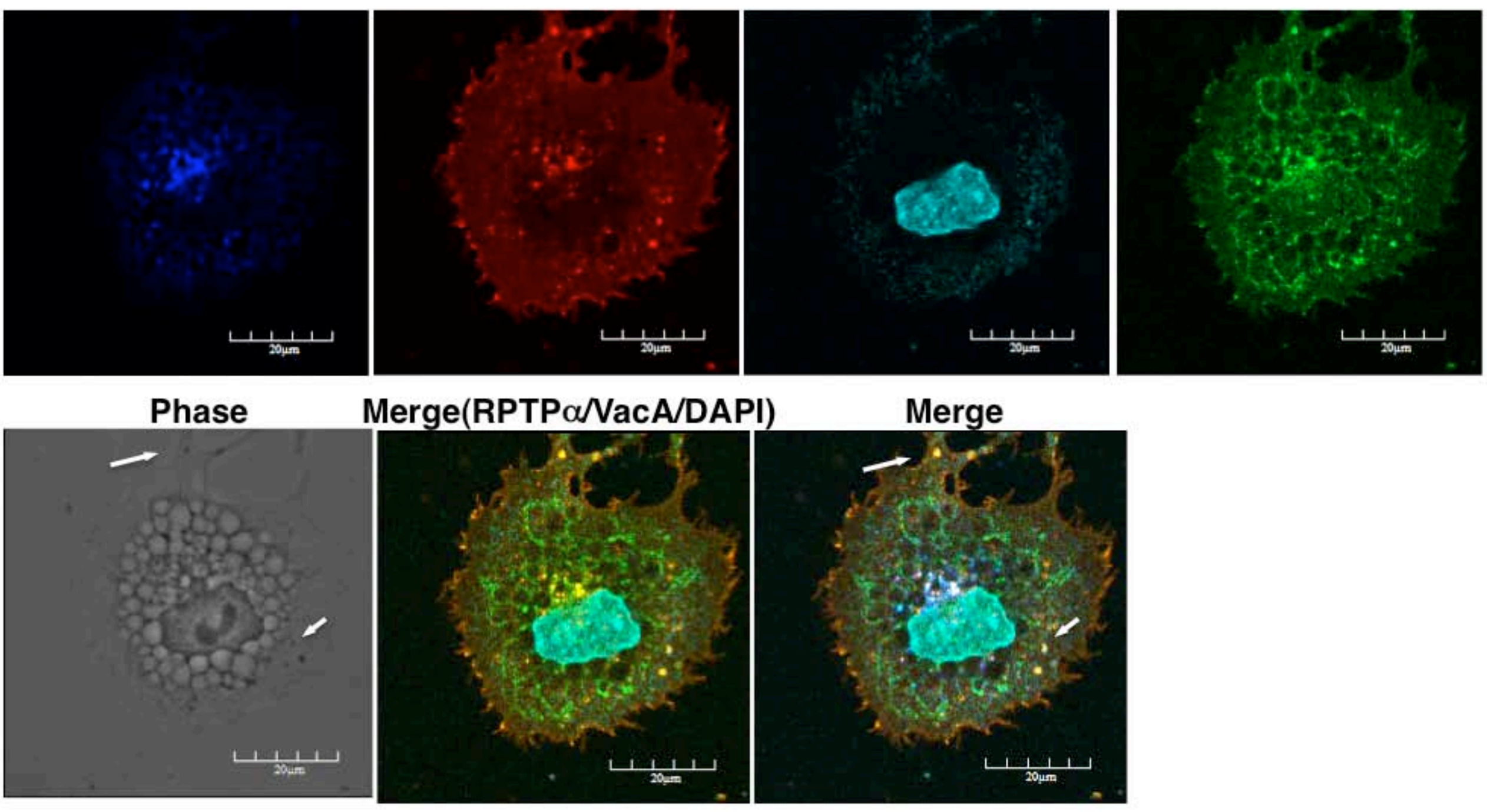
LC3B
Alexa555-VacA
DAPI
RPTPα
Phase
Merge(RPTPα/VacA/DAPI)
Merge
20μm

Fig. 5D

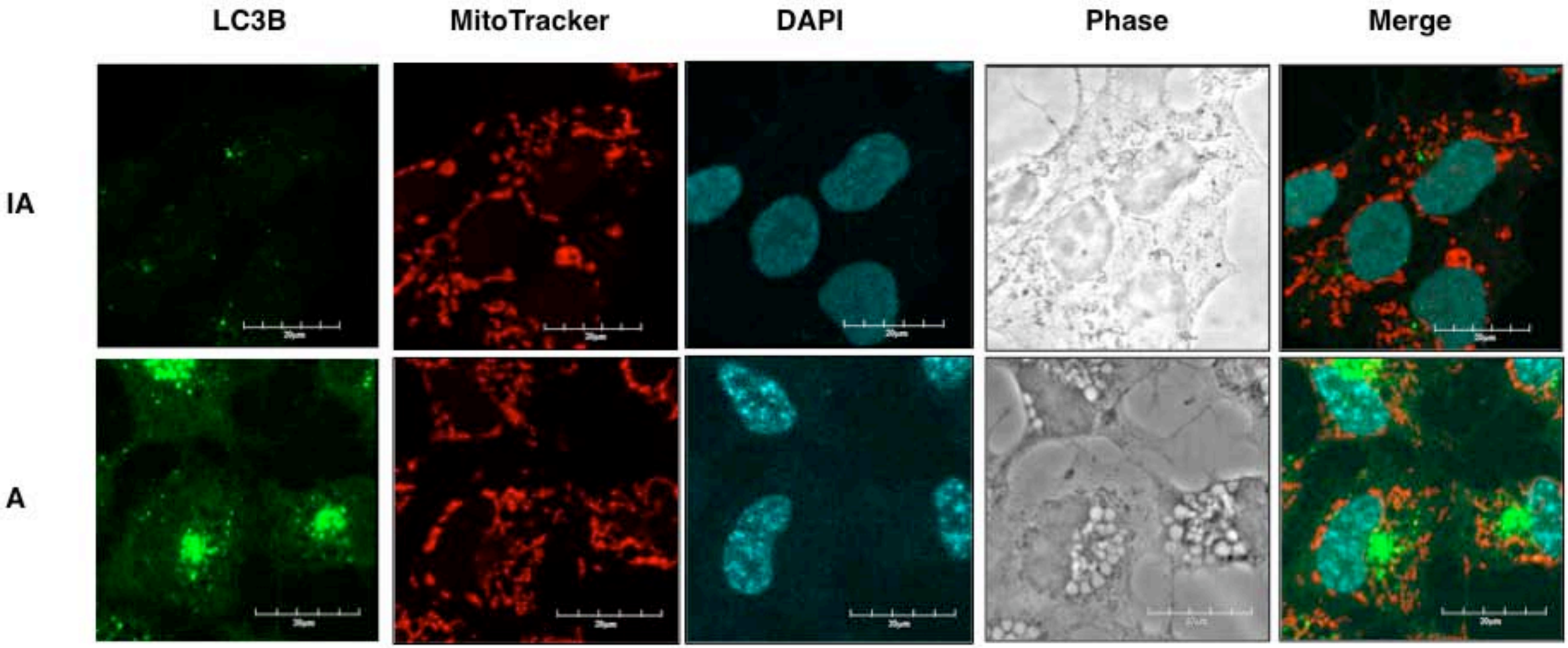

Fig. 5E

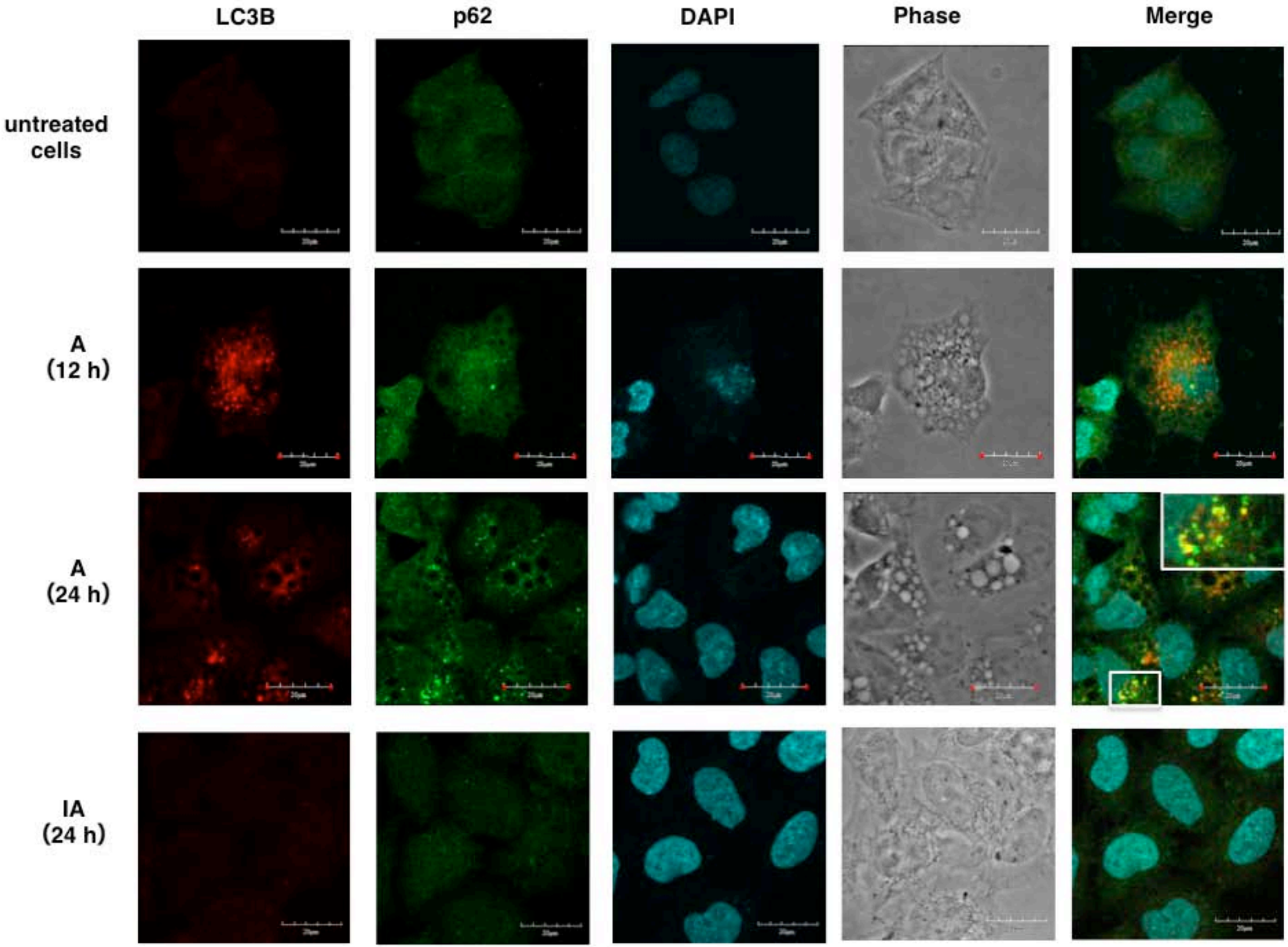

Fig. 6

a

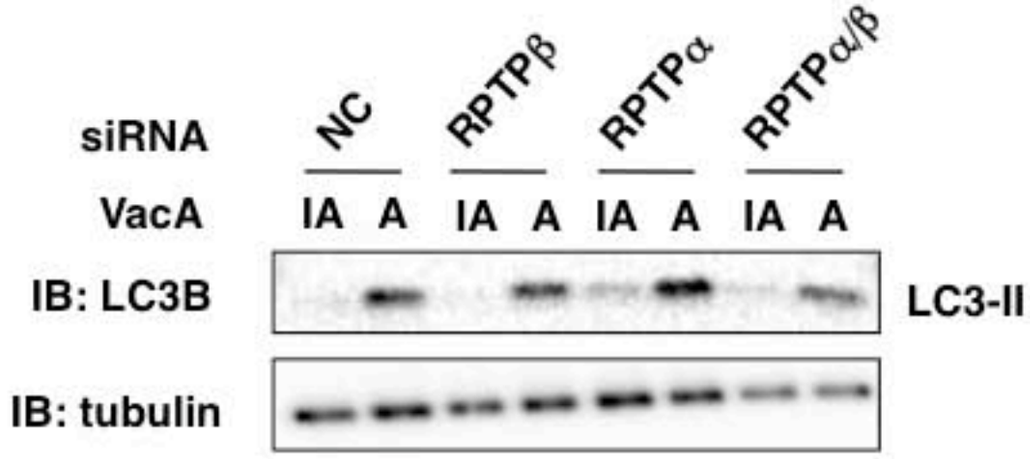
siRNA
NC
RPTPβ
RPTPα
RPTPα/β
VacA
IA A IA A IA A IA A
IB: LC3B
LC3-II
IB: tubulin

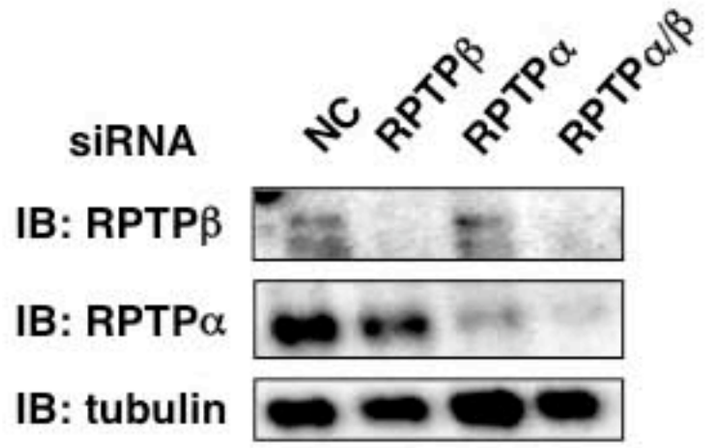
siRNA
NC
RPTPβ
RPTPα
RPTPα/β
IB: RPTPβ
IB: RPTPα
IB: tubulin

b

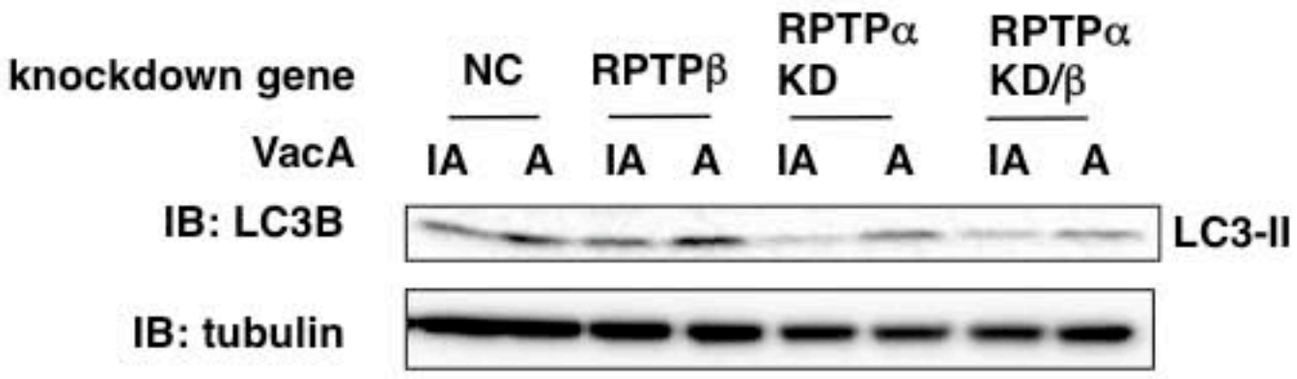
knockdown gene
NC
RPTPβ
RPTPα KD
RPTPα KD/β
VacA
IA A IA A IA A IA A
IB: LC3B
LC3-II
IB: tubulin

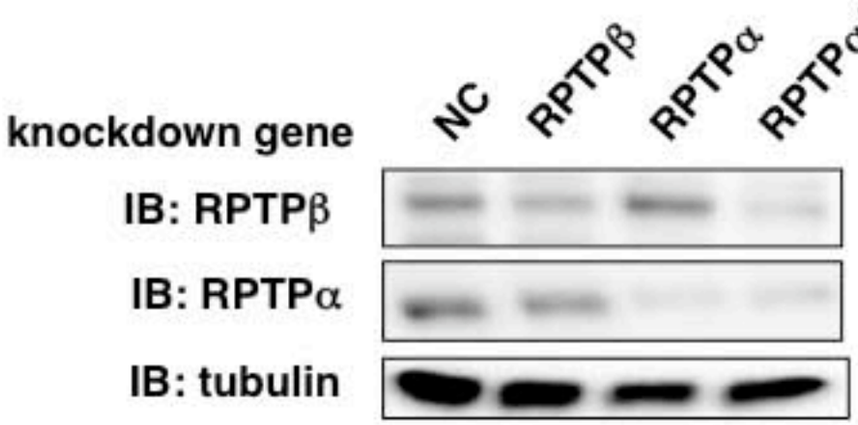
knockdown gene
NC
RPTPβ
RPTPα
RPTPα/β
IB: RPTPβ
IB: RPTPα
IB: tubulin

c

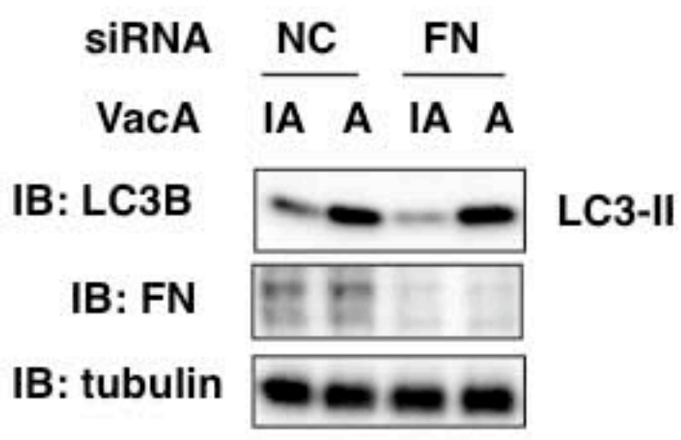
siRNA
NC
FN
VacA
IA A IA A
IB: LC3B
LC3-II
IB: FN
IB: tubulin

Fig. 7

a

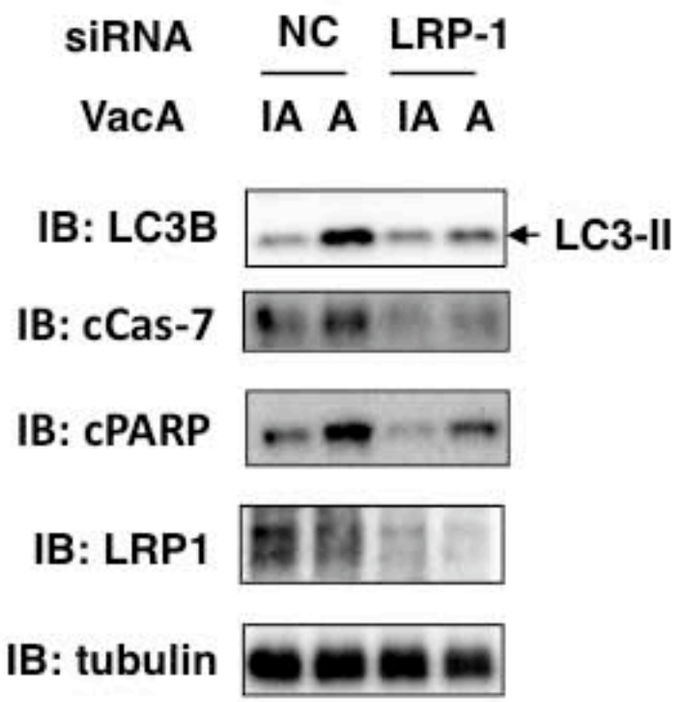
siRNA
NC
LRP-1
VacA
IA A IA A
IB: LC3B
LC3-II
IB: cCas-7
IB: cPARP
IB: LRP1
IB: tubulin

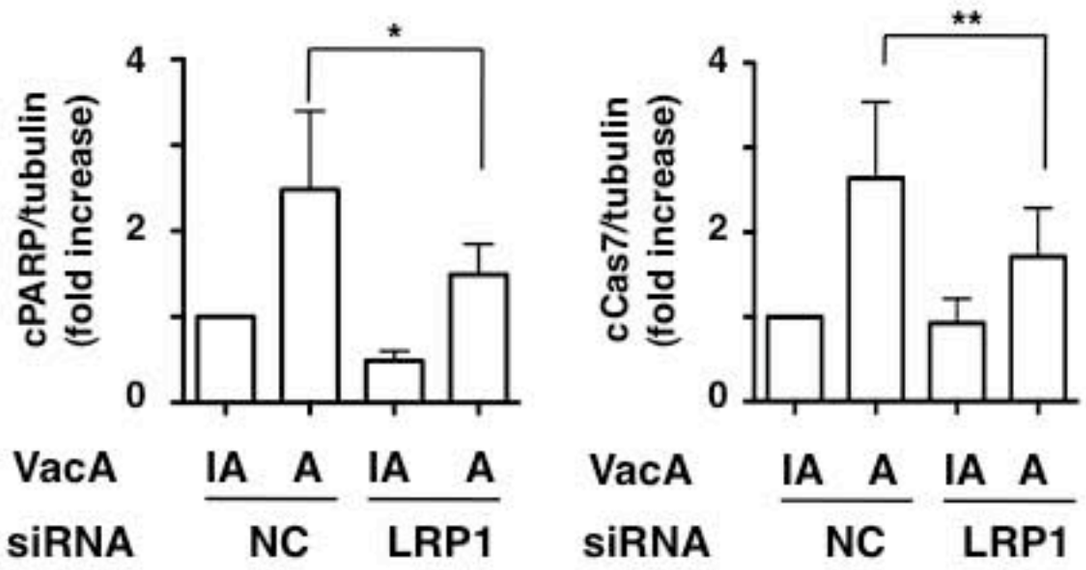
cPARP/tubulin (fold increase)
4
2
0
*
VacA
IA A IA A
siRNA
NC LRP1
cCas7/tubulin (fold increase)
4
2
0
**
VacA
IA A IA A
siRNA
NC LRP1

b

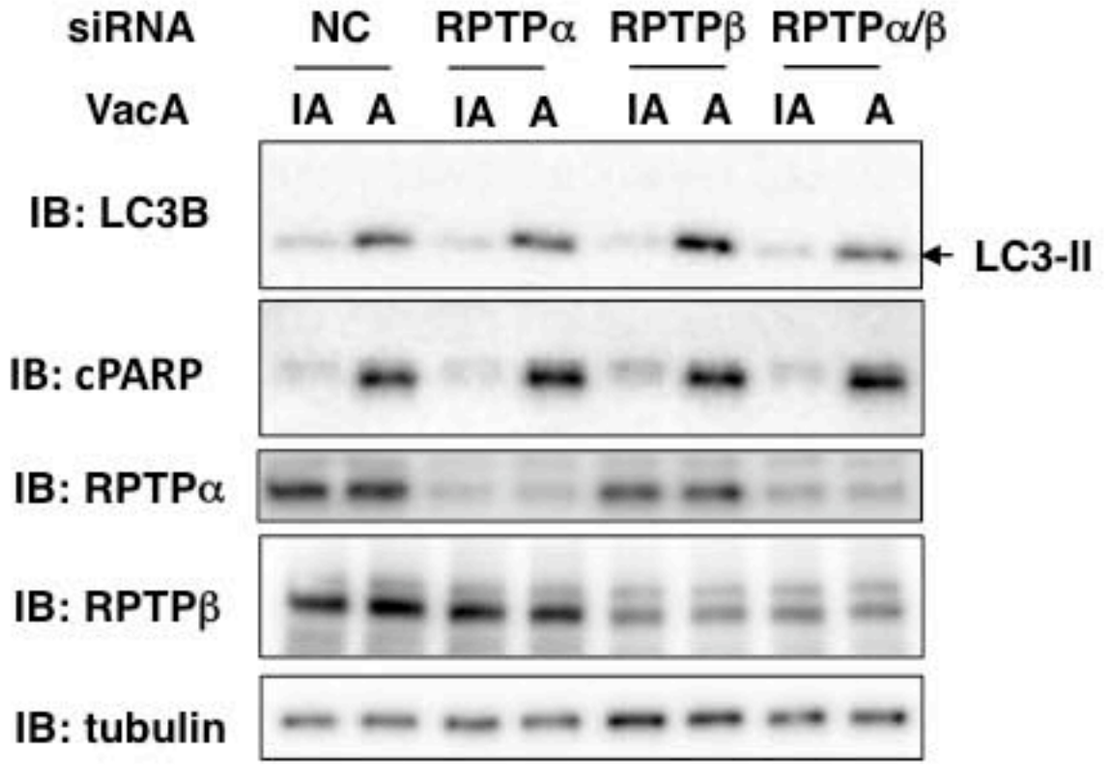
siRNA
NC
RPTPα
RPTPβ
RPTPα/β
VacA
IA A IA A IA A IA A
IB: LC3B
LC3-II
IB: cPARP
IB: RPTPα
IB: RPTPβ
IB: tubulin

Fig. 8

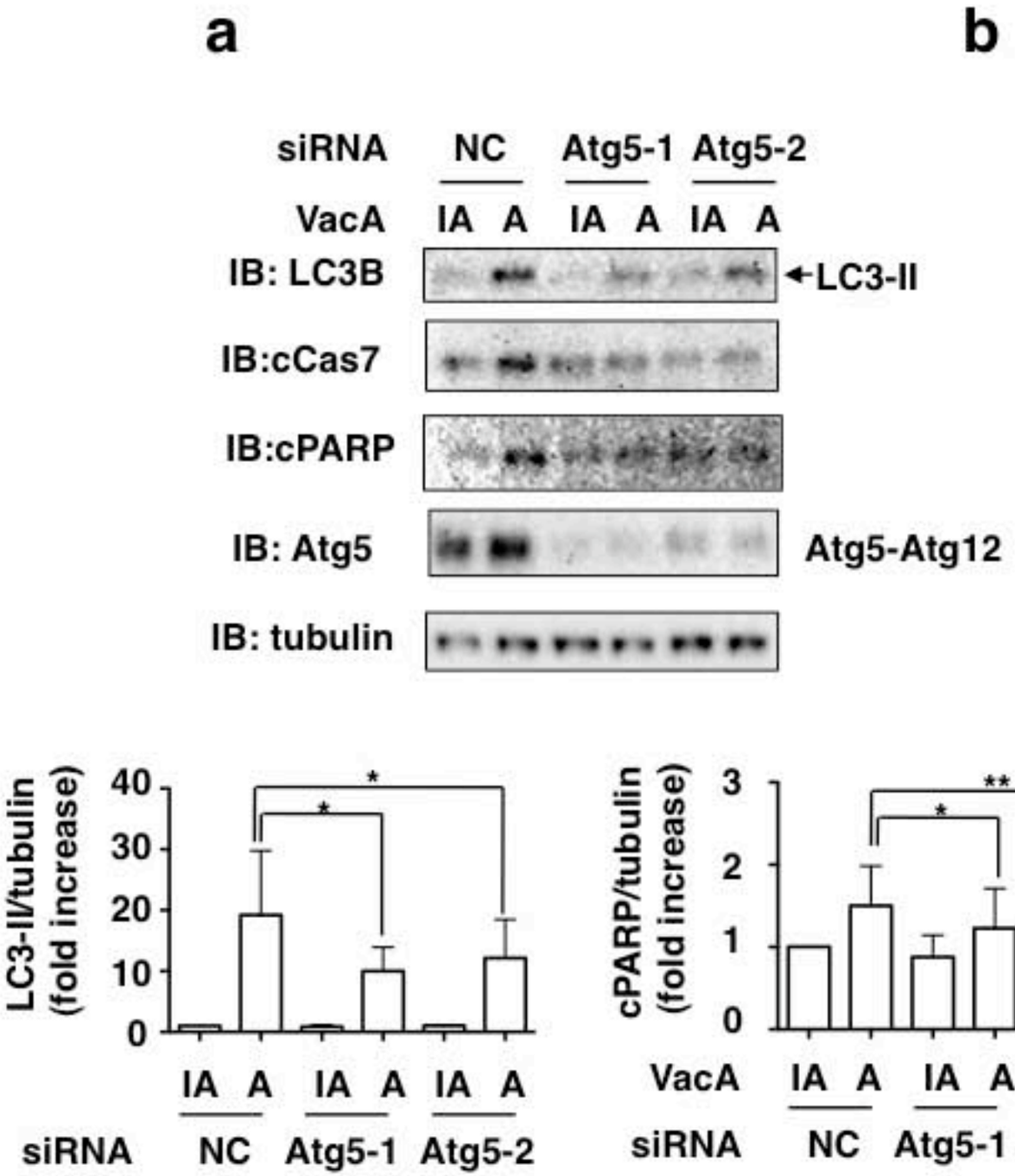
a
siRNA
NC
Atg5-1
Atg5-2
VacA
IA
A
IB: LC3B
LC3-II
IB:cCas7
IB:cPARP
IB: Atg5
Atg5-Atg12
IB: tubulin
LC3-II/tubulin (fold increase)
40
30
20
10
0
*
cPARP/tubulin (fold increase)
3
2
1
**


b
inhibitor
-
Z-VAD
Necrostatin
VacA
IA
A
IB: LC3B
LC3-II
IB: tubulin

Fig. 9

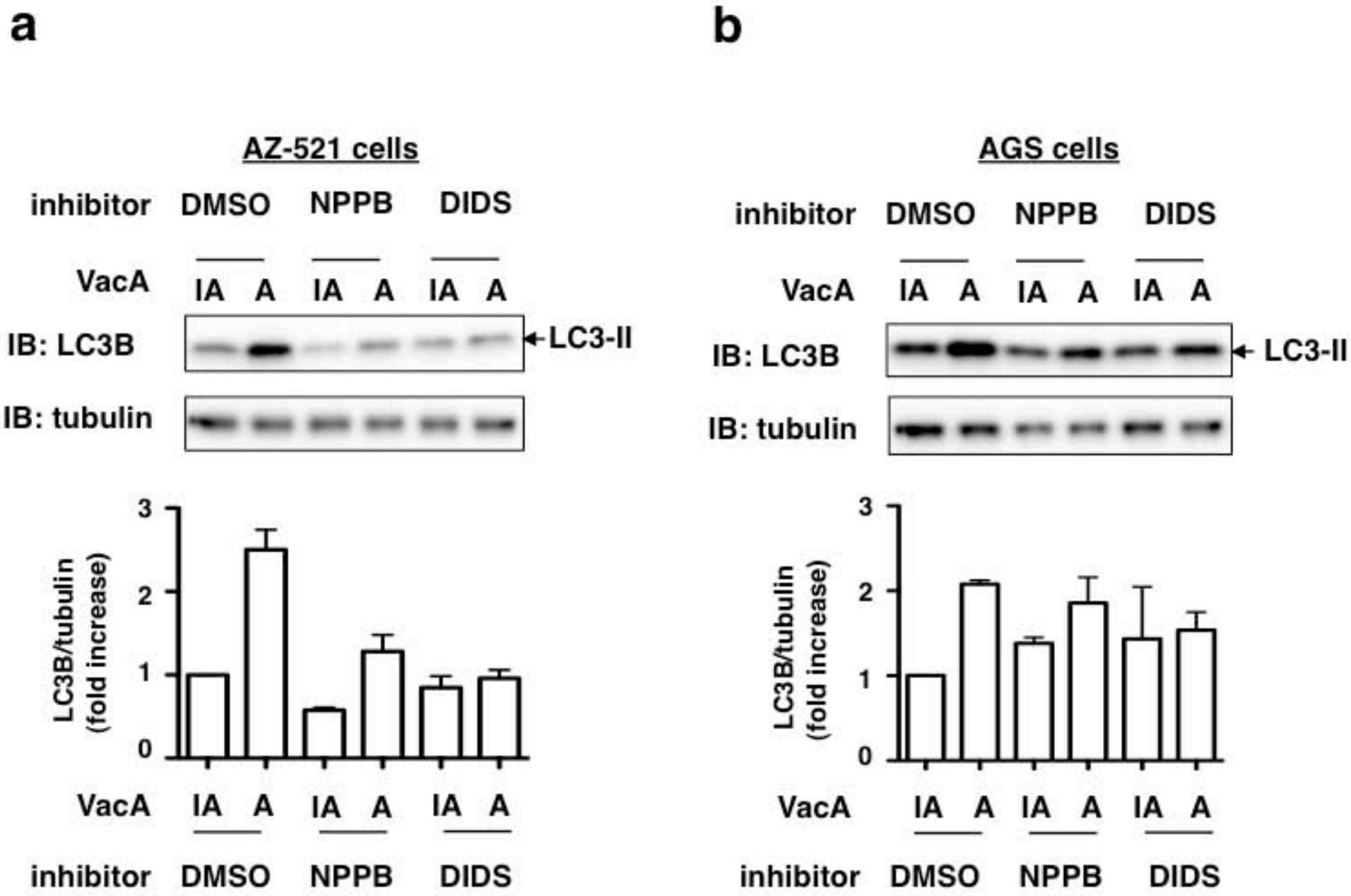
a
AZ-521 cells
inhibitor DMSO NPPB DIDS
VacA IA A IA A IA A
IB: LC3B
LC3-II
IB: tubulin
LC3B/tubulin (fold increase)
0
1
2
3
VacA IA A IA A IA A
inhibitor DMSO NPPB DIDS
b
AGS cells
inhibitor DMSO NPPB DIDS
VacA IA A IA A IA A
IB: LC3B
LC3-II
IB: tubulin
LC3B/tubulin (fold increase)
0
1
2
3
VacA IA A IA A IA A
inhibitor DMSO NPPB DIDS

Supplemental Information

Fig. S1

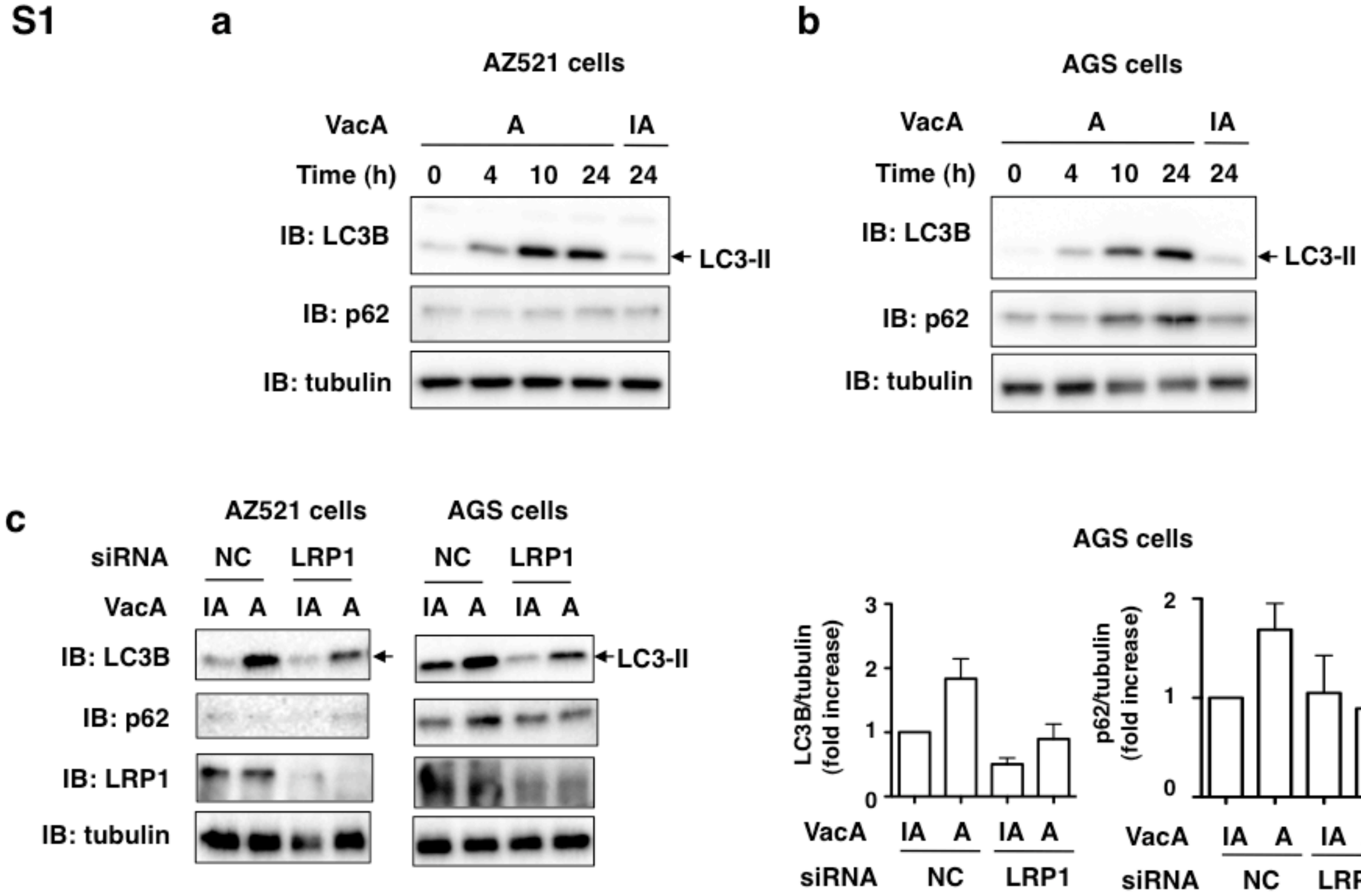

Supplemental Information

Fig. S2

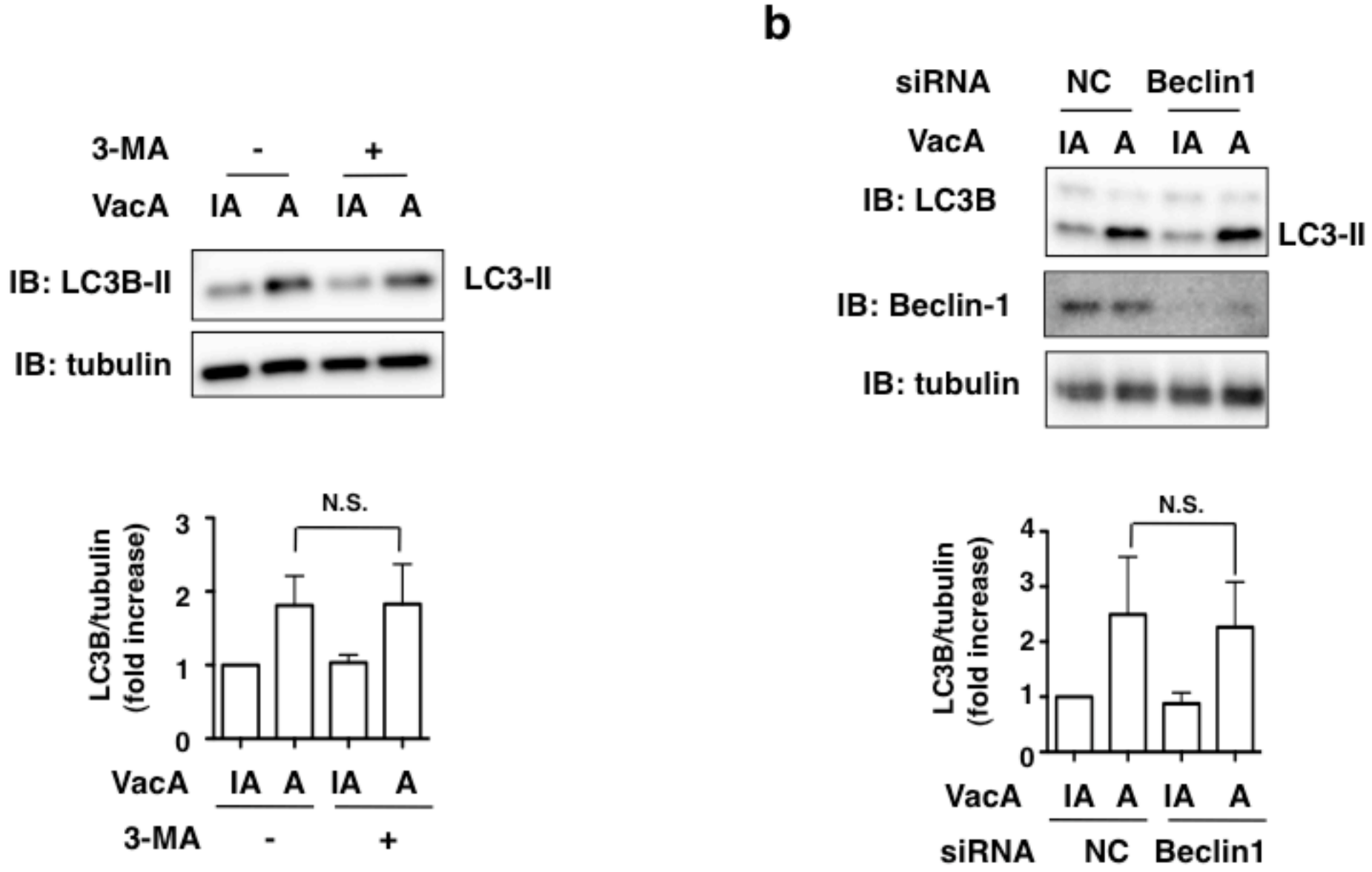

Supplemental data legends

Sup Figure 1 VacA induced p62 generation in a time-dependent manner. AZ521 (**a**) or AGS (**b**) cells were incubated with 120 nM heat-inactivated (IA) or wild-type VacA (A) for the indicated time points at 37 ^{o}C and the cell lysates were subjected to immunoblotting with anti-LC3B, anti-p62 or anti-α-Tubulin antibodies, which served as a loading control. A blot representative of two separate experiments is shown.

a. AZ-521 or AGS cells were incubated with 120 nM heat-inactivated (IA) or wild-type VacA (A) for 4 h at 37 ^{o}C and the cell lysates were subjected to immunoblotting with anti-LC3B, anti-p62, anti-LRP1 or anti-α-Tubulin antibodies. A blot representative of two separated experiments is shown. Quantification of VacA-induced LC3-II levels in the cells was performed by densitometry (right panel). Data are means and SD of values from two independent experiments.

Sup Figure 2. Effects of 3-MA and Beclin-1 silencing on VacA-induced LC3-II generation.

a. AZ-521 cells were pretreated with 1 mM 3-MA for 30 min at 37 ^{o}C and then incubated with 120 nM heat-inactivated (IA) or wild-type VacA (A) for 4 h at 37 ^{o}C. Cell lysates were subjected to immunoblotting with anti-LC3B antibody or anti-α-tubulin antibody as a loading control. A blot representative of three separate experiments is shown. Quantification of VacA-induced LC3-II levels in the cells was performed by densitometry (bottom panel). Quantification of VacA-induced LC3-II levels in AZ-521 cells was performed by densitometry (bottom panel). Data are presented as mean ±SD (n=3). N.S., not significant.

b. NC or Beclin-1 siRNA-transfected AZ-521 cells were incubated with 120 nM heat-inactivated (IA) or wild-type VacA (A) for 4 h at 37 ^{o}C and the cell lysates were subjected to immunoblotting with anti-LC3B or anti-Beclin1 antibodies. α-Tubulin served as a loading control. A blot representative of three separate experiments is shown. Quantification of VacA-induced LC3-II levels in the indicated siRNA-transfected AZ-521 cells was performed by densitometry (bottom panel). Data are presented as mean ±SD (n=3) . N.S., not significant.